Effect of Back Rake Angle and Shape of PDC Cutter On Wear Rate In Hard Formation

By

Kong Yien Yi

14956

Dissertation submitted in partial fulfilment of

the requirements for the

Bachelor of Engineering (Hons)

(Mechanical Engineering)

JANUARY 2015

Universiti Teknologi PETRONAS

32610 Bandar Seri Iskandar

Perak Darul Ridzuan

Malaysia

CERTIFICATION OF APPROVAL

**EFFECT OF BACK RAKE ANGLE AND SHAPE OF PDC CUTTER ON
WEAR RATE IN HARD FORMATION**

By

Kong Yien Yi

14956

A project dissertation submitted to the

Mechanical Engineering Programme

Universiti Teknologi PETRONAS

In partial fulfilment of the requirement for the

BACHELOR OF ENGINEERING (Hons)

(MECHANICAL ENGINEERING)

Approved by,

_____

(AP DR AHMAD MAJDI BIN ABDUL RANI)

UNIVERSITI TEKNOLOGI PETRONAS

32610 BANDAR SERI ISKANDAR,

PERAK DARUL RIDZUAN, MALAYSIA.

JANUARY 2015

CERTIFICATION OF ORIGINALITY

This is to certify that I am responsible for the work submitted in this project, that the original work is my own except as specified in the references and acknowledgements, and that the original work contained herein have not been undertaken or done by unspecified sources or persons.

_____

KONG YIEN YI

ABSTRACT

This project aimed to investigate the effect of cutter back rake angle and shape of cutter on Polycrystalline Diamond Compact (PDC) cutter wear rate in hard formation application. PDC bits are widely used to drill soft formations in petroleum industry due to their excellent Rate of Penetration (ROP). Conventional PDC bits often failed in hard formations due to the formation abrasiveness and impact load damage. Advancements in cutter technologies by enhancing the high wear and impact resistance helps to expand the PDC bit application. The study is focused on the single cutter test using 16mm PDC cutter. The drilling operation is carried out in granite formation under constant applied force and velocity. The theoretical basis of the PDC cutter is studied using the cutter-rock interaction model and Merchant's cutting model. A 3D simulation model of rock breaking using a single PDC cutter is established with Finite Element Method (FEA) based on elastoplastic mechanics and rock mechanics to analyze the stress beneath the cutter. The FEA model of the single cutter test is simulated using ABAQUS software. Effect of back rake angle and shape of PDC cutter on the rule of cutter wear rate are analyzed by using the wear theory. Result showed that 30˚ back rake angled cutter and beveled-shaped cutter are the best design to minimize the cutter wear rate in hard formation.

ACKNOWLEDGEMENT

TABLE OF CONTENTS

LIST OF FIGURES

LIST OF TABLES

APPENDICES

ABBREVIATIONS AND NOMENCLATURES

3D	*Three Dimensional*
CATIA	*Computer-Aided Three-Dimensional Interactive Application*
DOC	*Depth of Cut*
FEA	*Finite Element Analysis*
FYP	*Final Year Project*
IADC	*International Association of Drilling Contractor*
PDC	*Polycrystalline Diamond Compact*
ROP	*Rate of Penetration*
RPM	*Rotary Speed*
TCI	*Tungsten Carbide Insert*
UCS	*Unconfined Compressive Strength*
UTP	*Universiti Teknologi Petronas*
WOB	*Weight on Bit*

CHAPTER 1
INTRODUCTION

1.1 Background of Study

Drill bit is a tool that attached to the end of the drill string to remove and fail the rocks to get the petroleum resources in petroleum industry as shown in Figure 1.1. The main operating parameters for running a bit are rotary speed (RPM), Weight on Bit (WOB) and bit hydraulics. The drill bit types are mainly consisted of the fixed-cutter (FC) bits and roller cone (RC) bits.
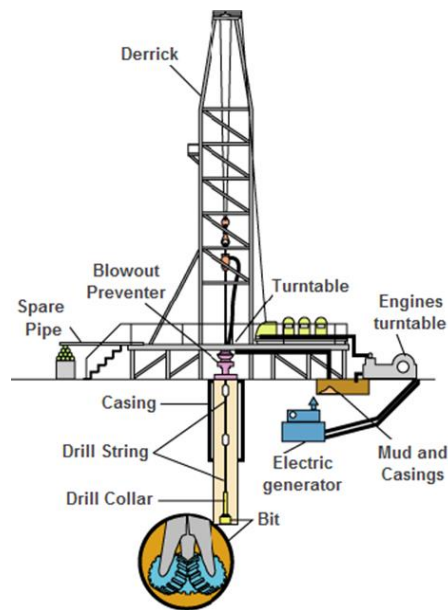
FIGURE 1.1 Drilling System

One typical example for FC bits is Polycrystalline Diamond Compact (PDC) bit (Figure 1.2) while Tungsten Carbide Insert (TCI) bit (Figure 1.4) is an example of roller cone. This project will be focusing on PDC bit only as PDC bit is widely used for soft formation drilling especially in Malaysia wells. The detailed components of a PDC bit are shown in Figure 1.3. Shearing action of PDC bit is acknowledged to have the highest cutting efficiency among all the drilling mechanisms. Thus, PDC bit cutting mechanism enables the bit to run with higher rate of penetration (ROP) than

the RC bit. However, the PDC bits are not applicable for hard, abrasive rock drilling. The bits can wear out easily due to the high temperatures and high impact forces.

FIGURE 1.2 PDC Drill Bit (Baker Hughes, 2012)
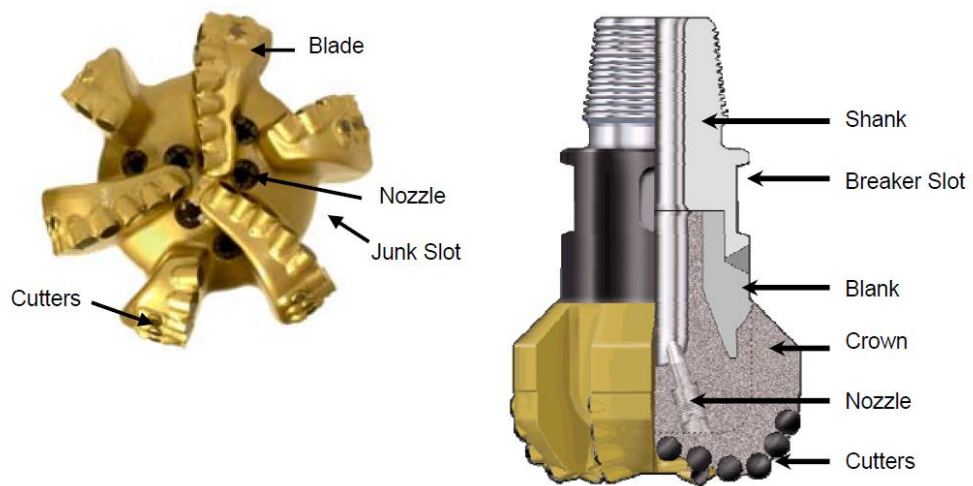
FIGURE 1.3 PDC Bit Face and Side View (Baker Hughes, 2012)
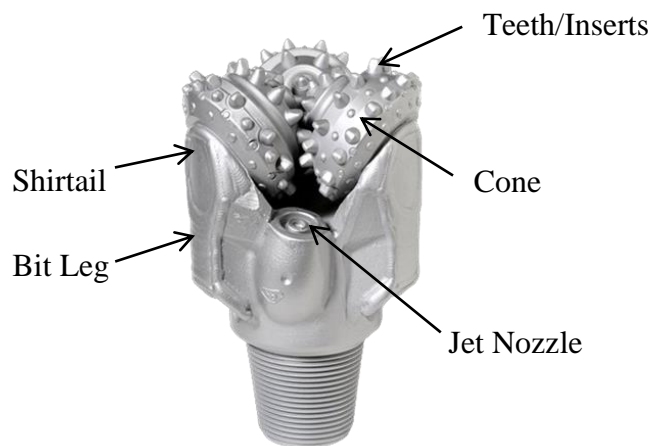
FIGURE 1.4 TCI Drill Bit (Baker Hughes, 2012)

The efficiency of drilling process is the major concern for all the drilling operations in petroleum industry. Bit performance (ROP and bit reliability) can be used to define the effectiveness of most of the drilling operations. An estimation and prediction of bit condition can help to optimize the bit performance, to maximize the drilling efficiency, to reduce the operational costs and to avoid catastrophic failure. Thus, bit wear remained as a critical issue in drilling. Thousands of bit types are developed for different applications to overcome this challenge.

Reduction of bit wear is essential to cut down the operational cost and to make sure the drilling is efficient. New bits suited for highly abrasive applications are developed to upgrade the bit durability. For example, tungsten carbide is introduced as the new PDC bit body material to enhance toughness and erosion resistance. These modifications enable the PDC bit to achieve higher ROP values and longer interval drilled. Two approaches are taken to optimize the performance of bit. Most of the bits are diagnosed using simulation software to check for the potential structural deficiencies. In addition, offset wells data are used as the guidelines to predict and evaluate the potential performance for next run.

The author would like to propose with a method to analyze the PDC cutter designs on the wear rate especially when drilling in hard formation using FEA model and wear model. The design parameters of the PDC bit are back rake angle and shape of the PDC cutter. Both analytical and simulation models are used to get the stress distributions on the bit. This method is more economical and less time-consuming compared to laboratory or field test. Changing and improvement in the cutter pattern can be easily done using FEA based on the requirements. The rock properties and the operating parameters are included in the model to obtain more accurate outputs. This can help to determine the best PDC cutter design with the maximum durability for hard formation applications.

1.2 Problem Statement

In Offshore Qatar, drilling the 311.55mm (12.25 in) hole section through Hith-Khaith formation with Unconfined Compressive Strength (UCS) of 35MPa to 205MPa is problematic. In Kurawit, drilling 16-in hole section with abrasive Zubair sand, Ratawi shale and hard carbonates (Jurassic formations) as shown in Figure 1.5 is challenging (Hussein et al., 2013). The high UCS and abrasive sandstone and siltstone structures in Egypt's Western Desert oil fields cause many drilling problems.
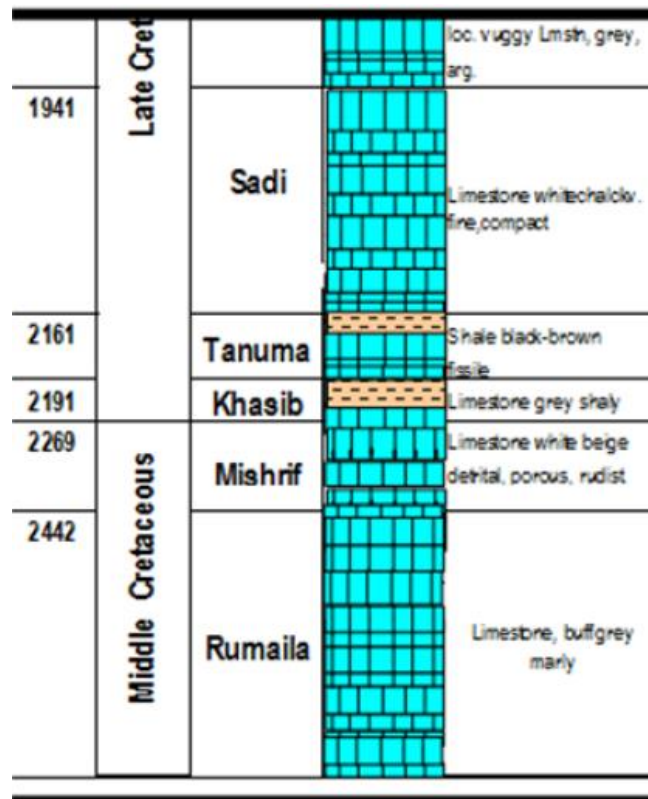
FIGURE 1.5 Lithologies of Zubair oil field (Hussein et al., 2013)

Conventional PDC bits are often failed in these applications due to the formation abrasiveness and impact load damage. This is an area where PDC bit under-performs as compared to roller cone bit. A more wear-resistant and abrasion-resistant cutter technology is needed to enhance the PDC bit application. Attention focused on the back rake angle and shape of the cutter which significantly influenced the bit durability in hard formation. To accomplish the objective, the back rake angles and shape of the cutter are altered and guided by the FEA based model to determine the PDC bit design that are best suited for hard formation.

1.3 Objectives

The specific objectives of this project are:

- To understand the behavior of the PDC cutter through analytical model.
- To simulate the stress beneath the PDC cutter with different designs.
- To analyze the effect of PDC cutter designs on cutter wear rate through the wear theory.
- To determine the PDC cutter designs to minimize wear rate in hard formation application.

1.4 Scope Of Study

This project intends to study the effect of the PDC cutter designs on wear rate in hard formation to determine the best design for the PDC bit in term of durability. The two cutter designs studied in this project are back rake angle and shape of the PDC cutter. The study focuses on the single cutter test in granite formation under constant applied external forces and velocity. The selected cutter size is 16mm and the cutter material is polycrystalline diamond (PCD) bonded with tungsten carbide-cobalt (WC-Co).

CHAPTER 2
LITERATURE REVIEW

1.1 Bit Wear

In manufacturing, wear is defined as the materials loss or erosion because of the action done on the surface. Wear rate is the amount of tool materials loss per unit distance cut by Li and Hood (1993). In petroleum industry, the PDC bit wear is explained using the International Association of Drilling Contractor (IADC) fixed cutter dull grading system as shown in Table 2.1. The common dull characteristics on PDC bit are listed in the Table 2.2. On the other hand, Liu et al. (2014) suggested that bit wear rate can be estimated from the loss of the cutter volume and the reduction of blade height. Many elements such as drilling hydraulics, bit patterns, mechanical parameters and rock properties have impacts on the performance of the bit runs. Liu et al. (2014) categorized these factors into uncontrollable and controllable groups.

A damaged or worn bit slows down the ROP, shortens the bit life and causes a poor hole quality (Cheatham and Loeb, 1985). The bit may require pulled out of the hole and replace with a new bit. Among all the dull conditions, broken teeth (Figure 2.1), lost cutters (Figure 2.2), worn teeth, erosion (Figure 2.3) are the major issues faced by PDC bit operations in Malaysia. The main reasons for the cutter failure were the poor wear resistance and poor impact toughness of Tungsten Cobalt (WC-Co) carbide which could not withstand harsh working environment at bottom hole (Tian et al., 2014).

TABLE 2.1 IADC dull grading system (Baker Hughes, 2012)

IADC Dull Grading System Chart							
Cutting Structure				B	G	Remarks	
Inner Rows	Outer Rows	Dull Characteristics	Location	Bearing Seals	Gauge $^1/_{16}''$	Other Characteristics	Reason Pulled
2	6			X			

TABLE 2.2 PDC Dull Characteristics

BT - broken teeth/cutters	LN - lost nozzle
BU - balled up	LT - lost teeth/cutters
CR - cored	NO - no major/other dull characteristics
CT - chipped teeth/cutters	PN - plugged nozzle/flow passage
ER - erosion	RO - ringout
HC - heat checking	WO - washed out
JD - junk damage	WT - worn teeth/cutters
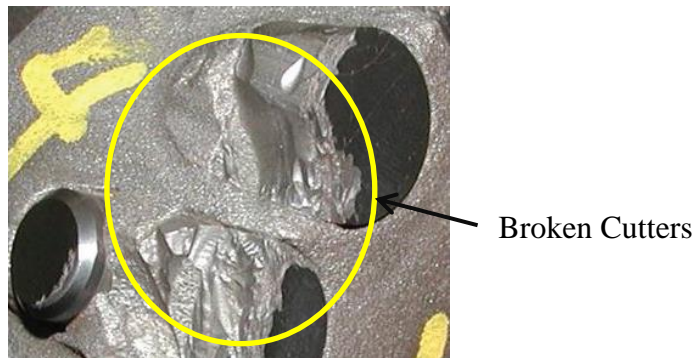
FIGURE 2.1 Broken Teeth (Baker Hughes, 2012)
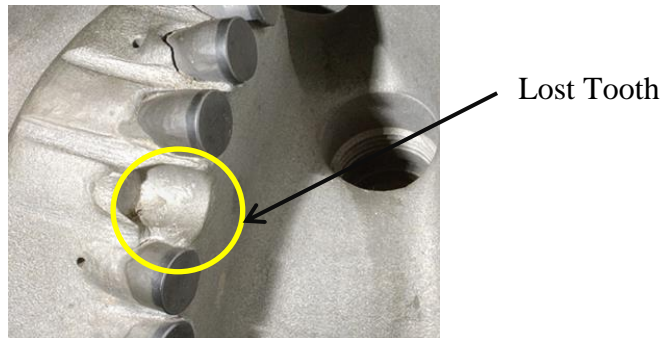
FIGURE 2.2 Lost Cutter (Baker Hughes, 2012)
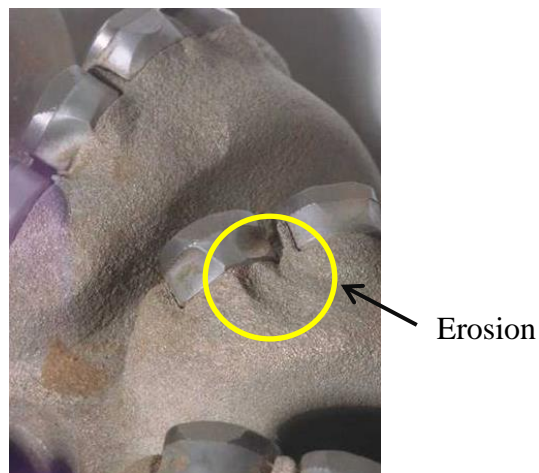
FIGURE 2.3 Erosion (Baker Hughes, 2012)

7

2.2 Formation Properties

As mentioned, one of the uncontrollable elements that affect the bit durability is the rock properties. Different rock formations behave differently when under pressure. Figure 2.4 shows the behavior of different rocks under the influence of pressure. Some rocks have complex behaviors, such as the granite, marble and sandstone. Understanding this behavior is important when doing application analysis and selecting bits. Rock can be broken or failed easier under unconfined condition. The strength of the rock increases rapidly and requires higher amounts of force to break under the influence of pressure. The inclination of mud weight used indicates the influence of pressure in drilling operation.
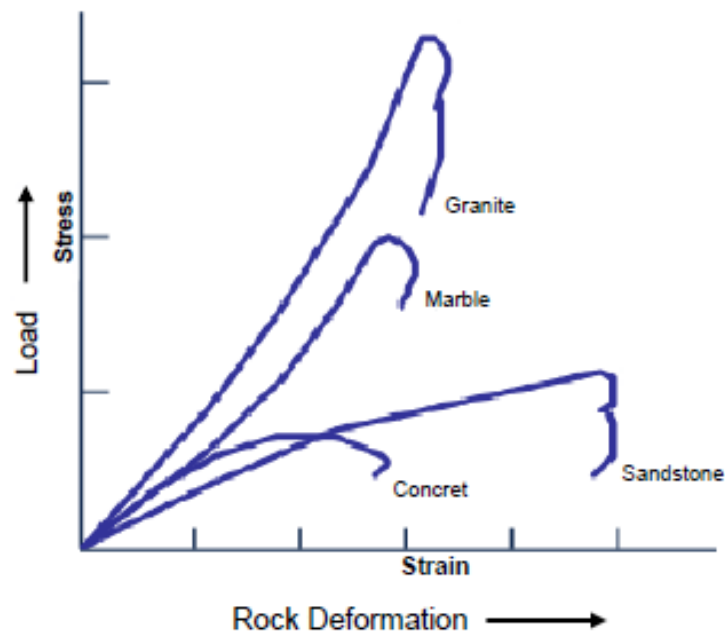
FIGURE 2.4 Stress and Strain Curve for Rocks

The oil field formations on the world can be categorized into seven groups by using the Unconfined Compressive Strength (UCS) values as the indicator. UCS is the pressure or force, applied over an area, required to break the rock at atmospheric pressure (Maute, 2005). Acoustic (DT) is used by HCC to estimate lithology and UCS since it is directly related to the porosity, an increase of which weakens the rock. Lithology estimation can be further refined and improved with additional log data: Bulk Density (RHOB), Neutron Porosity (NPHI), Photoelectric (PE), and Shear Sonic (DTs). Basically, bit wear is not a problem in soft formation but a critical issue

in hard formations. Cutter types will cross application boundaries according to specific formation characteristics, and operating environment as tabulated in Table 2.3.

The PDC cutter fails the rock through shearing; this is a cutting action where the direction of the load and the resulting fracture are roughly parallel. As the cutter penetrates the formation, the tip of the cutter shears and removes the formation in layers. Current PDC bit are generally safe for soft rock application with UCS values in the range of 0 – 170 MPa (0 – 25000 psi). In general terms, hard rock was deemed non-drillable by PDC bits. However, hard, abrasive rocks (i.e. chert, dolomite or metamorphic rocks) could not be avoided in some of the operations. These undesirable rock properties may result in severe bit damage and wear. Thus, the next challenge is to model PDC bit with good reliability to penetrate faster and further especially in extremely hard formation with UCS values more than 240 MPa (35000 psi) (Henry et al., 2011).

Granite is a common type of igneous rock that can be found on the earth's surface. The compositions of granite are primarily quartz and feldspar, followed by small amounts of others minerals like mica and amphiboles. This is one of the hard rock formations which are commonly used for the testing of new PDC cutter technology since it is easily available. The UCS value of graphite is varied from 100 MPa to 300MPa (14500 psi to 43500 psi).

TABLE 2.3 Generalized Cutter Recommendations (Baker Hughes, 2012)

Rock Hardness	Unconfined Compressive Strength (UCS)	Rock Type	Recommended Cutter Type
Ultra Soft	< 25 MPa (4000 psi)	Gumbo Shale, Clay, Unconsolidated Sand	PDC
Soft	25 – 55 MPa (4000 – 8000 psi)	Chalk, Salt, Anhydrite, Shale, Shaly Sandstone	PDC
Soft to Medium	55 – 100 MPa (8000 – 15000 psi)	Shale, Limestone, Marl, Sandstone	PDC Ballaset
Medium	100 – 125 MPa (15000 – 18000 psi)	Shale, Siltstone, Sandstone, Limestone	PDC Ballaset
Medium to Hard	125 – 170 MPa (18000 – 25000 psi)	Shale, Siltstone, Sandstone, Limestone, Dolomite	PDC Ballaset Natural Diamond Impregnated
Hard	170 – 240 MPa (25000 – 35000 psi)	Shale, Siltstone, Sandstone, Limestone, Dolomite	(PDC) Ballaset Natural Diamond Impregnated
Extremely Hard	> 240 MPa (35000 psi)	Sandstone, Chert, Quartzite, Volcanic, Igneous, Metamorphic	Natural Diamond Impregnated

2.3 PDC Cutter

The reliability of the PDC drill bit life is greatly dependent on the PDC cutter. In order to improve bit performance and durability across a wider range of lithologies, the advancements in PDC cutter technology are essential. A PDC cutter (Figure 2.5) consists of a diamond table with many synthetic diamonds and a cemented tungsten carbide substrate (backing) that are bonded together. PDC bit is in removing rock is dependent on several factors. Increased rock hardness reduces bit cutter life. The number of cutters, the back rake and other design features of the cutter will also affect cutter life. Furthermore, the material of the cutter and design of cutter material affects bit cutter life (Hareland, 2009). The diamond table of each conventional PDC cutter is designed to have a 45 º edge chamfer. Rounding the edge of the cutter and increasing the sintering pressures under cutter manufacturing enables the cutter to be more thermally stable and abrasion-resistant when drilling in hard formations.
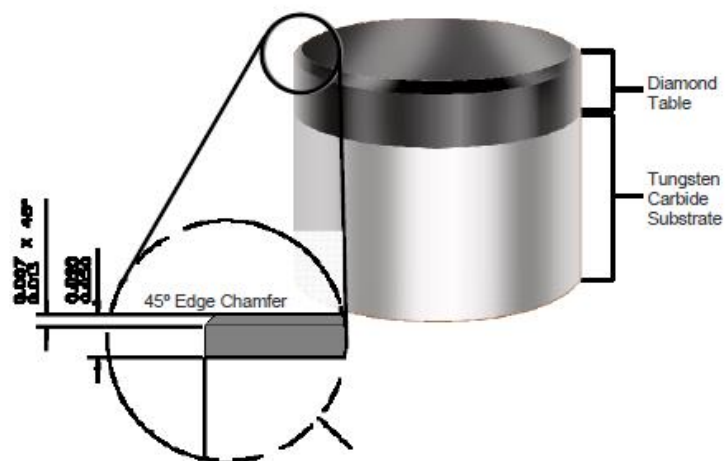
FIGURE 2.5 PDC Cutter

Four common cutter sizes available on market are 19mm, 16mm, 13mm and 8mm. Bit size helps to determine the cutter size chosen. The 19mm cutter generates largest cuttings and has most usable diamond height. The 16mm and 13mm can be applied in wide range of bit sizes. The 8mm is used in small diameter bit to provide design flexibility. Smaller PDC cutters do not provide a tougher bit as they have less available volume. The PDC cutter's toughness and durability are dependent on the impact resistance and abrasion resistance. The impact resistance of the cutter is greatly affected by diamond table composition, table thickness, the carbide substrate

and the cutter's edge chamfer. On the other hand, the key cutter factor that determines abrasion resistance is the diamond table composition. For instance, fine diamond grain size cutters, such as 10 μm, provides less abrasion than those from coarse diamond grains (Hareland, 2009). Thus, in order to improve PDC bit life in hard rock applications, the question to be addressed is how the design of the PDC cutter reduces the bit wear.

2.3.1 Back Rake Angle

Back rake angle (Figure 2.6) is the negative rake angle to the formation based on the position of PDC cutters on the PDC drill bit. It defined the angle made by the cutter face and a line perpendicular to the hole bottom (Rajabov, et al., 2012). Thus, back rake angle also determines the bit-rock interaction. The aggressiveness and durability of a bit are greatly dependent on the back rake angle. In soft formation, a lower back rake angle such as 15 ° would be a preferable choice as the durability is less of a concern. A less aggressive back rake angle such as 30 ° is mostly used in the upper shoulder to provide bit durability and reduce bit vibration by reducing the cutter failure from impact loading. Higher back rakes reduce the wear flat sizes they generate at specific IADC dull grades (Wilmot, 2003). Due to the increase of the back rake angle, it makes the effective cutting edge length increases and the cutting area and cutting arc length decrease, which significantly reduces rock-breaking efficiency but improves the bit durability.

Less cutter back rake reduce durability but increases ROP

Greater cutter back rake increases durability but slows ROP
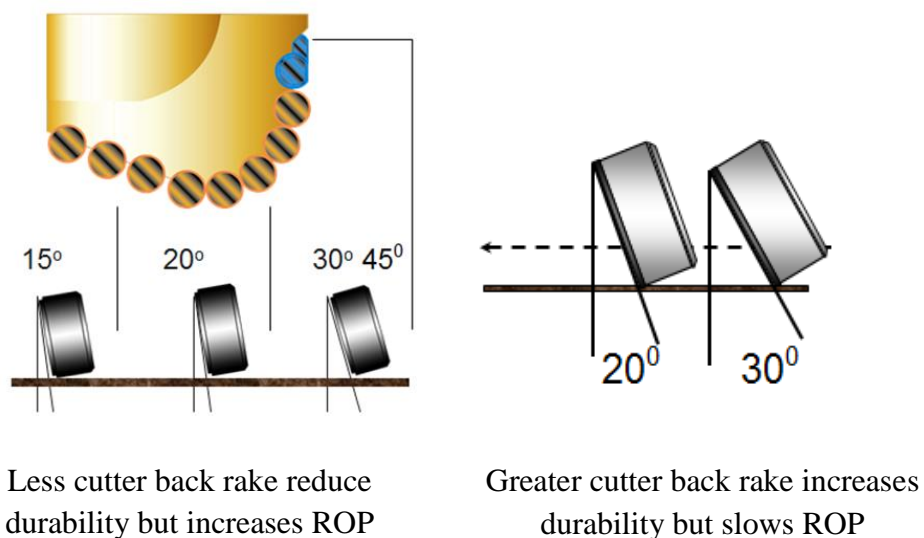
FIGURE 2.6 Back Rake Angle (Baker Hughes, 2012)

2.3.2 Shape of Cutter

For the ease of arrangement of cutters on given bit profile, cylindrical-shaped cutters are commonly used in conventional PDC bit to maximize the cutter densities. The residual stresses inside the cutters can be reduced by modifying the interface between the diamond table and backing. This can help to maximize the impact resistance of the PDC cutter. Specialized cutter shapes (Figure 2.7) are designed to improve the bit durability in hard formations. Cutter with beveled-shaped diamond table has a lower aggressiveness and effective back rake angle for specific formations. Higher total diamond volume is expected to improve the bit durability, and thus longevity and drill interval (Wilmot, 2013).
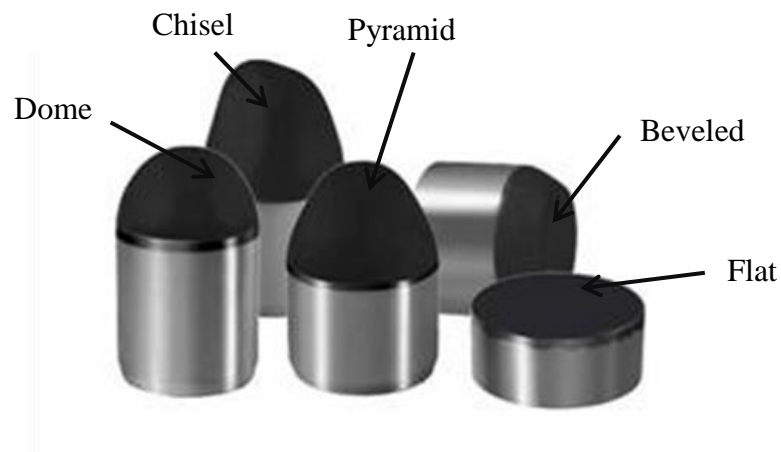
FIGURE 2.7 Shapes of the Cutters (Baker Hughes, 2012)

2.4 PDC Bit Operating Parameters

The operating parameters for PDC bits are not as closely linked together as they are for tricone bits. A high specified weight on bit does not require a correspondingly low rotary speed, and does not necessarily reduce the number of hours that the bit can be run before becoming un-acceptably worn (Forbes, 2012). In some circumstances, it can actually increase the run duration, if the higher weight stabilizes the bit and stops bit whirl.

2.4.1   Weight On Bit (WOB)

PDC bits do not need as much weight as tricone bits, and usually cannot tolerate as much weight as can a tricone bit. The weight on bit range that a PDC bit can apply related to the cutter diameter and count. A PDC bit with 13 mm diameter cutters can normally be operated with between 115 and 227 kg (250 and 500) lbs weight per cutter. The equivalent weights per cutter are 68 to 136 kg (150 to 300 lbs) for 8 mm diameter cutters, and 158 to 318 kg (350 to 700 lbs) for 19 mm diameter cutters (Forbes, 2012).

2.4.2   Rotary Speed (RPM)

According to Forbes (2012), the rotary speed at which PDC bits can operate is not directly related to the weight on bit. They can typically accept higher rotary speeds than tricone bits. Abrasive wear rates of PDC cutters increase with increasing cutter speed. Cutter speeds increase directly proportional to the cutter's distance from the bit's center of rotation. This means that the maximum advisable rotary speed for a given formation tends to be lower for larger diameter bits than it is for smaller bits.

2.5 Methods Used to Estimate Drilling Efficiency

2.5.1 PDC Bit Analytical Model

A lot of studies have been done to predict the effectiveness of drilling experimentally or theoretically. PDC analytical modelling methods was the most popular method used to understand how well a PDC bit could perform. To configure a FC model, single-cutter experiments need to be conducted first and integrate the data for modelling. The first PDC model, "Merchant's metal cutting model" was developed by Warren and Sinor (1986) to predict the cutter conditions and forces with the detailed inputs (i.e. formations, ROP, RPM and bit geometry). Followed by Glowka (1986 & 1987), he produced a model to evaluate the depth of cut (DOC) and then came out with a "PDCWEAR" code to predict grades of the cutters. However, this study is limited to the soft rock drilling only. These two models were not able to predict the ROP values as the ROPs were used as an input.

Estimation of ROP was then proposed by the model of Hareland and Rampersad (1994) and by correlating the ROP with the operating parameters. Motahhari's (2008) model was able to predict ROP and evaluate wear rate of the PDC bit. However, bit hydraulics effect was not considered in his study and this affected the accuracy of the results. Furthermore, Yahiaoui et al. (2012) also conducted a single cutter test through the measurement of the capabilities of drilling and wear rate to design a PDC model. However, the main purpose of this study was to highlight the material properties that have a significant effect on the cutter quality.

The weakness of the analytical method is that the laboratory or field data are required to generate the model. Besides, the FC models are limited to the fixed conditions and the accuracy of the estimation is greatly dependent on the assumptions.

2.5.2 Analytical Model Coupled With Data Analytics

According to Liu et al. (2014), it was really hard to predict the bit quality due to the unpredictable down-hole conditions. None of the existing model could describe the precise bit damage. Thus, both the mathematical model and the real-time data should be integrated to suppress the uncertainties of downhole conditions. This method can refine the accuracy of the ROP and bit grade estimations as real gamma ray (GR) data was used as an input to represent the well-bore condition. However, this approach required much higher cost and time consuming to obtain the real GR data.

2.5.3 Neural Network

Neural Networks was created for the prediction of outputs for drilling operations (i.e. ROP values and mainly the bit quality) by Bilgesu et al. (1997). The drilling data generated by simulator were used to establish the relationship between the complex patterns. This method has been tested using real-time data and proved to be more accurate than the drag-bit models. This is because the neural network includes all the important operating parameters (i.e. bit hydraulics, mechanical parameters, formation properties) as the inputs to simulate the operations. However, the applicable of the network was limited to the hardness of the rocks and the types of bit.

2.5.4 Finite Element Analysis (FEA)

FEA model was used by Mohd Noor (2014) to simulate the PDC bit runs in multi-layer formations. He used the CATIA software to create the designs followed by ANSYS Explicit Dynamics to simulate the drilling operation. The four main features of bit were being modified to study their effects on the ROP and the best combination of the designs is determined. This method is cost-effective as no laboratory data are required and there is no limitation in the bit types. However, the bit state and bit hydraulics are not considered as the variables in this study. In real world, the effect of bit wear and bit hydraulics on drilling operations cannot be ignored since these variables influence the bit performance significantly. Fear (1999) also mentioned that bit wear state is a controllable factor that has a bad impact on the ROP.

2.6 Analytical Model

2.6.1   Cutter-Rock Interaction Modelling

Rajabov, et al. (2012) and Che et al. (2012) developed a new 3D analytical PDC cutter-rock interaction model by considering the effect of back rake angles, side rake angles and the coefficient friction of rock. The horizontal cutting force of the cutter with a given the normal force can be predicted if the back rake angle of the cutter and the rock coefficient of friction are known. The static balance of forces acting externally on a single PDC cutter during cutter-rock interaction is used to develop an analytical model. The free diagram is shown in Figure 2.8. The external forces acted are:

- Cutting Force – F_c, acting perpendicular to the cutter surface
- Friction Force, F_{fc}
- Wear Force, F_w, acting perpendicular to the cutter wear flat at the bottom
- Wear Frictional Force, F_{fw}

The shearing and friction between the cutter and crushed rock resulted in these forces. Thus, the equations below can be obtained from the balance of external cutter forces:

$$F_H = F_C \cos\alpha \cos\beta - F_{fc} \sin\alpha \cos\beta + F_{fw} \tag{1}$$

$$F_S = F_C \cos\alpha \sin\beta - F_{fc} \sin\alpha \sin\beta \tag{2}$$

$$F_N = F_C \sin\alpha - F_{fc} \cos\alpha + F_w \tag{3}$$

where F_H is the horizontal force, F_S is the shearing force, F_N is the normal force, α is the back rake angle and β is the side rake angle, and

$$F_c = R_c A_c, \ F_{fc} = \mu F_c = \mu R_c A_c \tag{4}$$

$$F_w = R_p A_w, \ F_{fw} = \mu F_w = \mu R_p A_w \tag{5}$$

R_c and R_p are the rock resistance to shearing and rock compressive strength in pounds per square inch (psi) respectively, A_c and A_w are the cutter-rock contact area and cutter wear area and μ is the coefficient of friction.
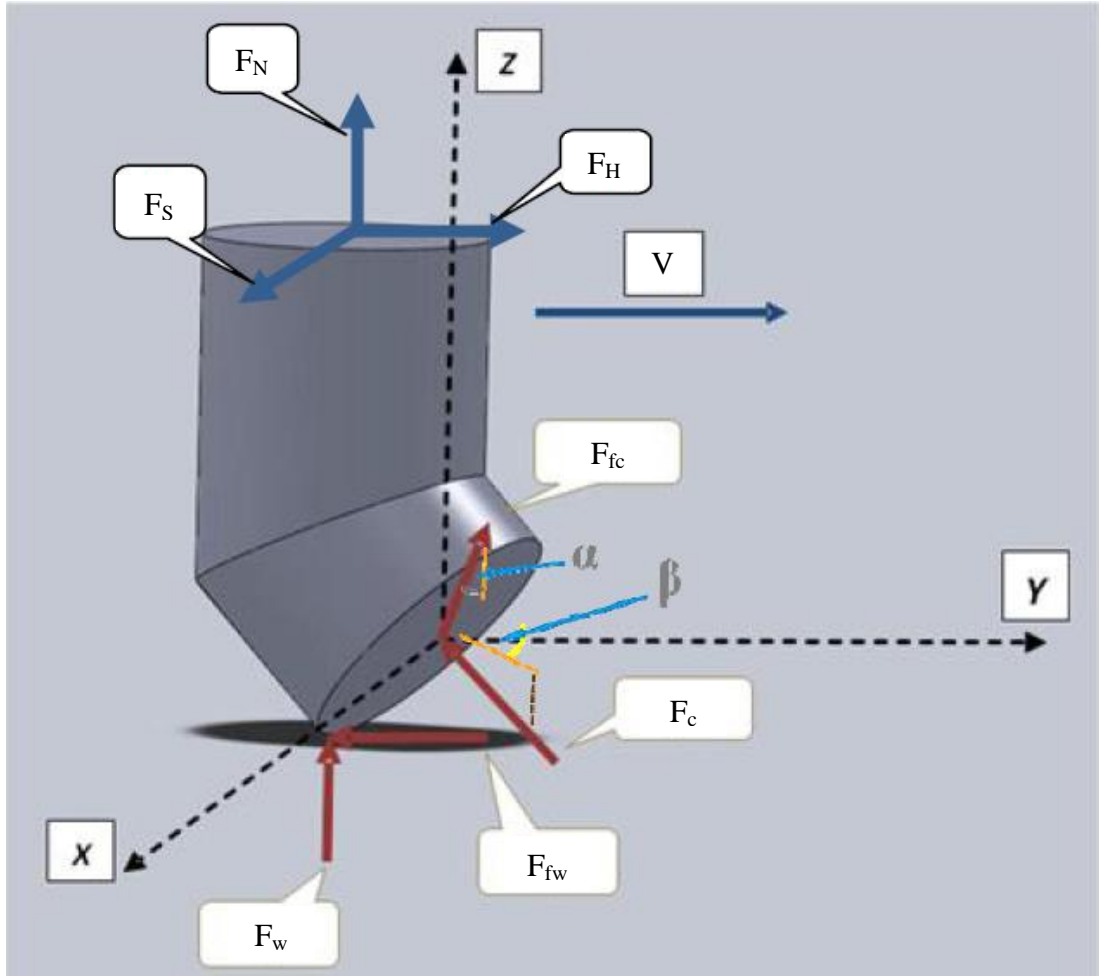
FIGURE 2.8 Free Body Diagram for Cutter-Rock Interaction

By applying the values of F_{fc} and F_{fw} from the equation (4) and (5) into equation (1), (2) and (3). The equation can be yielded respectively:

$$F_c - \mu F_c \tan \alpha = \frac{F_H - \mu F_W}{\cos \alpha \cos \beta} \tag{6}$$

$$F_c - \mu F_c \tan \alpha = \frac{F_S}{\cos \alpha \sin \beta} \tag{7}$$

$$F_c + \mu F_c \cot \alpha = \frac{F_N - F_W}{\sin \alpha} \tag{8}$$

From equation (8), μF_c can be obtained as:

$$\mu F_c = \frac{F_N - F_W}{\cos \alpha} - F_c \tan \alpha \tag{9}$$

By substituting the equation (8) into equation (6) and doing some arrangement, equation (10) is obtained:

$$F_c = \frac{F_H + F_N \tan \alpha \cos \beta - F_W(\mu + \tan \alpha \cos \beta)}{\cos \alpha \cos \beta (1 + \tan^2 \alpha)} \tag{10}$$

Assuming the cutter is new, thus the wear force is negligible. In this case, the equation (10) can be simplified in the form:

$$F_c = \frac{F_H + F_N \tan \alpha \cos \beta}{\cos \alpha \cos \beta (1 + \tan^2 \alpha)} \tag{11}$$

If the coefficient of friction is known, the equation (11) can be derived in the form:

$$F_c = \frac{F_N}{\sin \alpha - \mu \cos \alpha} \tag{12}$$

If there is no wear at the cutter, and substitute F_c from equation (12) into equation (1), the equation (13) is obtained:

$$F_H = F_N \cos \beta \left[\frac{1 - \mu \tan \alpha}{\mu + \tan \alpha} \right] \tag{13}$$

Equation (14) is the 3D analytical model that predicts the horizontal cutting force if the normal force and coefficient of friction is known by considering the effect of back rake and side rake angles. If the side rake angle ($\beta = 0$), the equation (13) is simplified to 2D form:

$$F_H = F_N \left[\frac{1 - \mu \tan \alpha}{\mu + \tan \alpha} \right] \tag{14}$$

This equation is the same as Kuru and Wojtanowinz's mode (1986).

2.6.2 Merchant's Model of Orthogonal Cutting

Merchant's cutting model is based on the principle of minimum energy. According to Merchant's model, a shear of material, and a friction between a tool and a chip are the two phenomena are responsible for the cutting force. The cutting force has been distributed on the shear force or the friction force. Starting from the first analytical cutting theory for metal cutting processes developed by Merchant, many cutting theories have been proposed to predict the loading forces at the tool–rock interface during rock cutting (Che, et al., 2012). The effects of stress distribution and failure criteria on loading force variations are being emphasized.

There are few assumptions for Merchant orthogonal cutting model (Juneja, Sekhon, and Seih, 2003):

- The cutting edge is a straight line extending perpendicular to the direction of motion, and it generates a plane surface as the work moves past it.
- Sharp tool edge.
- The deformation is experienced by the workpiece across a thin shear plane.
- The workpiece is rigid and perfectly plastic.
- The shearing surface is a plane extending upward from the cutting edge.
- The chip does not flow to side.
- The depth of cut is constant uniform relative velocity between work and tool.
- Continuous chip, no built-up-edge.

The force circle diagram of merchant's model is shown in Figure 2.9. The terminologies for the diagram are listed below.

- Cutting Force – F_c
- Thrust Force – F_t
- Friction Force – F
- Normal Frictional Force – N
- Shear Force – F_s
- Normal Shear Force – F_n

- Resultant Force - R
- Rake Angle – α
- Shear Angle – ϕ
- Feed Velocity – V
- Frictional Angle – τ

FIGURE 2.9 Force Circle Diagram of Merchant's Model

By knowing the F_c, F_s, α, and ϕ, all other component forces can be calculated as:

$$F = F_C \sin \alpha + F_t \cos \alpha \qquad (15)$$

$$N = F_C \cos \alpha - F_t \sin \alpha \qquad (16)$$

The coefficient of friction will be then given as in equation (17):

$$\mu = \frac{F}{N} = \frac{F_C \sin \alpha + F_t \cos \alpha}{F_C \cos \alpha - F_t \sin \alpha} \qquad (17)$$

On shear plane,

$$F_s = F_C \cos \varphi - F_t \sin \varphi \qquad (18)$$

$$F_n = F_C \sin \varphi + F_t \cos \varphi \qquad (19)$$

Thus, the resultant force is derived as equation (20):

$$R = \sqrt{F_c{}^2 + F_t{}^2} = \sqrt{F_s{}^2 + F_n{}^2} = \sqrt{F^2 + N^2} \qquad (20)$$

The stress on the tool rake face can be obtained using the equation (21) and (22):

$$\sigma = \frac{\text{Normal Frictional Force}}{\text{Contact Area}} = \frac{N}{A} \qquad (21)$$

$$\tau = \frac{\text{Shear Force}}{\text{Contact Area}} = \frac{F}{A} \qquad (22)$$

2.6.3 Wear Model

Tangena (1987) proposed a wear model which indicates that the total tribological system determines the wear behaviour. Von mises stress is related to wear by calculating the wear volume per unit distance, W in μm^2 using equation (28):

$$W = k_2 V \bar{\sigma}^{\frac{1}{bn'}} \qquad (28)$$

where k_2 is an arbitrary wear constant, V is the deformed volume, $\bar{\sigma}$ is the von Mises stress in MPa, b is a constant whose value is approximately 0.5, and n' is the cyclic strain-hardening coefficient (Tangena, 1988). The magnitude of the von Mises stress depends on the contact geometry, the mechanical properties of the materials, the friction and the externally applied forces. This large value of this coefficient indicates that one system parameter, the von Mises stress in the stressed volume, is dominant in the wear process and will determine the wear. In the system, the volume of deformed material, V, *is* approximately equal to Π x a^2 x d, where a is the contact radius and *d* the thickness of the layer. Different values of the contact radius, a, is possible to exist at the same von Mises stress. Thus, there is no simple relation between the average von Mises stress and the contact radius. For simplicity, the volume of deformed material V is taken as constant compared to the von Mises stress to the power to construct the wear model as shown in Table 2.4.

TABLE 2.4 Ludwik Relationship of Different Materials (Tangena, 1988 and Schouwenaars et al., 2009)

Material	Constant, K (N/mm^2)	Strain-Hardening Coefficient, n′	Power, $\frac{1}{bn'}$	Proportionality Constant, k_2V
Gold (Au)	478	0.63	3.15	3.36×10^{-2}
Polycrystalline Diamond (PCD)	573	0.31	6.45	1.50×10^{-11}
Nickel (Ni)	4889	0.55	3.64	3.45×10^{-7}
Copper (Cu)	530	0.44	4.55	3.72×10^{-6}
304 Stainless Steel	1400	0.44	4.55	4.48×10^{-6}

CHAPTER 3

METHODOLOGY

3.1 Project Framework

The project framework is shown in the Figure 3.1.

> **DECIDE PARAMETERS:**
>
> I. Constant Variables: Applied Force, Feed Rate Size and Material of Cutter, Rock Properties (Granite)
>
> II. Independent Variables: Back Rake Angle and Shape of Cutter
>
> III. Dependent Variables: Cutter Wear Rate

> **METHOD SELECTION:**
>
> 1. The behaviour of the PDC cutter is studied using analytical model.
> 2. The PDC stress estimation is conducted using the Finite Element Analysis (FEA) method.
> 3. The PDC cutter and formation 3D models are produced using CATIA software and converted into iges format.
> 4. The FEA-based model is simulated using ABAQUS software.
> 5. The effect of back rake angle and shape of cutter on the cutter wear are analyzed by using the wear theory.

> **ANALYTICAL MODEL:**
>
> 1. An analytical model is used to compute the functional forces and stress of a cutter in a drilling operation.
>   a. Horizontal Force
>   b. Axial Stress
>   c. Shear Stress

FEA- BASED MODEL:

1.   Details of the simulation:

    a. The materials properties of the PDC cutter and granite formation are defined.

       i.   Johnson-Cook Damage

      ii.   Damage Evolution

     iii.   Density

     iv.   Elastic

      v.   Plastic

    b. The parts are assembled and meshed after defining the element size and element type of each component.

       i.   PDC Cutter – 0.5, 3D Stress

      ii.   Granite Formation - 0.05, Cohesive

    c. The explicit dynamic integration method is selected as the step and the time period is set to 60s.

    d. The interaction and constraints of the models are defined.

       i.   Interaction – Tangential behavior (Penalty)

    e. The load on the bit is defined as body force.

       i.   Horizontal Force

      ii.   Normal Force

    f. The boundary conditions for the model are defined.

       i.   Velocity/Angular velocity (PDC Cutter)

      ii.   Symmetry/Antisymmetry/Encastre (Granite Formation)

    h. Result of the simulation:

       i.   Von Mises Stress

DATA COLLECTION AND DATA ANALYSIS:

1. The result from the simulation is validated and verified.

2. The relationship between stress and wear rate is established using wear model.

3. The effect of back rake angle and shape of cutter on the wear rate in hard formation is studied.

FIGURE 3.1 Research Methodology
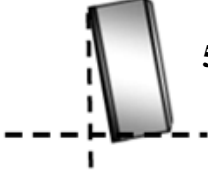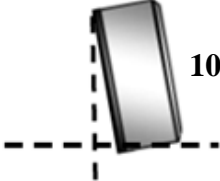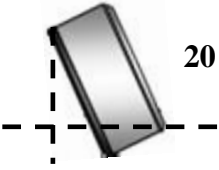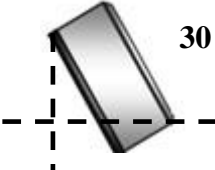
3.2 PDC Single Cutter Test

The theoretical basis of the PDC cutter is studied using the general mechanical model. A 3D simulation model of rock breaking using a single PDC cutter is established with Finite Element Method (FEA) based on elastoplastic mechanics and rock mechanics to analyze the stress distribution on the cutter. The designs of PDC cutter on the rule of cutter wear rate are analyzed by using the wear theory. The two cutter design parameters studied are back rake angle and shape of cutter. 3D models of PDC cutter are drawn using CATIA software.

3.2.1   Back Rake Angle

The back rake angles studied are 0˚, 5˚, 10˚, 15˚, 20˚ and 30˚ as shown in Table 3.1.
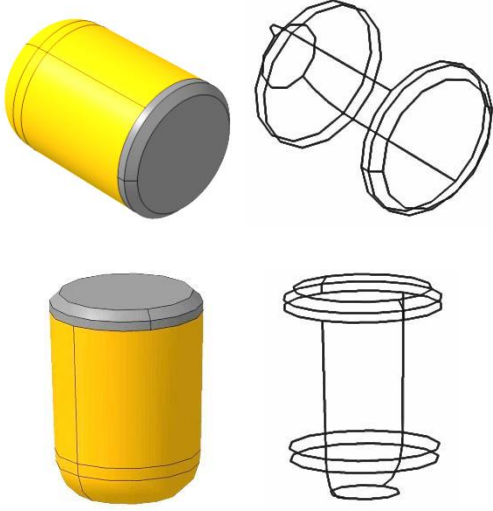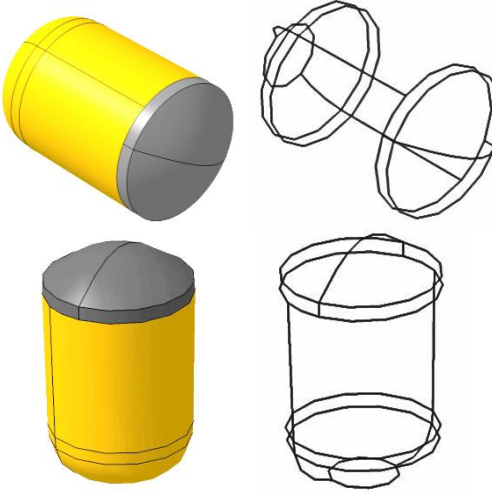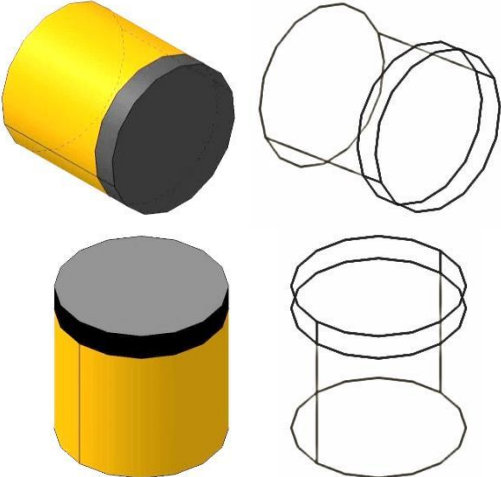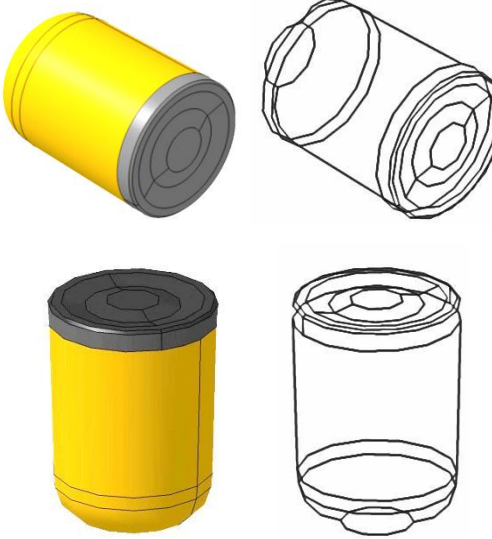
TABLE 3.1 Back Rake Angle

0 degree	5 degree
0˚	5˚
10 degree	15 degree
10˚	15˚
20 degree	30 degree
20˚	30 ˚

3.2.2 Shape of Cutter

The shapes of cutter studied are beveled, conical, flat and multidimensional as shown in Table 3.2.

TABLE 3.2 Shape of Cutter

Beveled	**Conical**
Flat	**Multidimensional**

3.2.3 Constant Parameters

The other design parameters of PDC cutter are kept as shown in Table 3.3.

TABLE 3.3 Constant Design Parameters for PDC Cutter

Polycrystalline Diamond Compact (PDC) Cutter	
Constant Parameter	*Variable*
Size of Cutter	16 mm
Material of Cutter	Polycrystalline Diamond (PCD) bonded with tungsten carbide-cobalt (WC-Co)
Diamond Carbide Interface	Conventional
Side Rake Angle	0 °

Table 3.4 shows the mechanical parameters that used to define the boundary condition for single cutter simulation.

TABLE 3.4 Mechanical Parameters for Single Cutter Test

Mechanical Parameter	*Variable*
Horizontal Force (F_H)	2500 N
Velocity	0.306 m/s

3.2.4   Model Parameters

3.2.4.1 Model Parameters of PDC Cutter

The material of PDC cutter is controlled with Johnson Cook law and plastic strain was adopted to judge the cutter damage. All the parameters of PDC cutter needed for the simulation is listed in Table 3.5.

TABLE 3.5 Model Parameters of PDC Cutter (Wesrling et al., 2010 & Yahiaoui et al, 2012)

	PCD	WC-Co
Material Parameters	*Parameter Values*	
Density, ρ (kgm^{-3})	3510	15000
Young's Modulus, E (GPa)	890	579
Poisson Ratio	0.07	0.22
Shear Modulus, G (GPa)	545	280
Strength Parameters	*Parameter Values*	
A (MPa)	4000	770
B (MPa)	500	177
n	0.14	0.12
Damage Parameters	*Parameter Values*	
D1	0.05	0
D2	1.873	0.33
D3	-2.272	-1.50
Thermal Parameters	*Parameter Values*	
Thermal Conductivity, k (Wm^{-1}K^{-1})	543	100
Specific Heat, C$_p$ (Jkg^{-1}K^{-1})	790	230
Thermal Expansion Coefficient, α (10^{-6}K^{-1})	2.5	5.2

3.2.4.2 Model Parameters of Rock Formation

The rock cutting test is conducted in granite formation. The constitutive relation of rock is controlled with Johnson Cook law and plastic strain was adopted to judge the rock breaking. All the parameters of granite formation needed for the simulation is listed in Table 3.6.

TABLE 3.6 Model Parameters of Rock Formation (Gao, et al., 2010 & Robertson, 1988)

Granite	
Material Parameters	*Parameter Values*
Unconfined Compressive Strength, UCS (MPa)	300
Density, ρ (kgm^{-3})	26200
Ultimate Tensile Strength, UTS (MPa)	256
Shear Yield Stress, τ_{yield} (MPa)	132
Young's Modulus, E (GPa)	70
Poisson Ratio	0.30
Kinetic Coefficient, μ_k	0.45
Strength Parameters	*Parameter Values*
A (MPa)	0.79
B (MPa)	1.60
c	0.007
Damage Parameters	*Parameter Values*
D1	0.040
D2	1.000
Thermal Parameters	*Parameter Values*
Specific Heat, C_p (Jkg^{-1}K^{-1})	790
Thermal Expansion Coefficient, α (10^{-6}K^{-1})	7.9
Thermal Conductivity, k (Wm^{-1}K^{-1})	4.0

3.3 Gantt Chart and Key Milestone

Table 3.7 and Table 3.8 show the gantt chart and key milestone for FYP I and FYP II.

TABLE 3.7 Gantt Chart and Key Milestone for FYP I

No	Activities/Week	1	2	3	4	5	6	7	8	9	10	11	12	13	14
1	Topic Selection	▓													
2	Preliminary Research Work on PDC Bit Wear		▓	▓	▓	▓									
3	Literature Review		▓	▓	▓	▓	▓	▓	▓	▓	▓	▓	▓	▓	▓
4	Method Selection					●									
6	KSB Field Trip							●							
5	Software Learning			▓	▓	▓	▓	▓	▓	▓	●				
7	3D Drawings Generation								▓	▓	▓	▓	▓	●	
8	Determination of Parameters											▓	▓	●	
9	Cutting Simulation in Hard Formation													▓	▓

TABLE 3.8 Gantt Chart and Key Milestone for FYP II

No	Activities/Week	1	2	3	4	5	6	7	8	9	10	11	12	13	14
1	Single Cutter Simulation in Hard Formation	▨	▨	▨	▨	▨	▨								
2	Phase 1 Simulation						●								
3	Phase 2 Simulation							●							
4	Data Collection and Data Analysis								▨	▨					
5	Pre-SEDEX										●				
6	SEDEX											●			
7	Wear Rate Determination												▨	▨	
8	Best PDC Cutter Design Determination														●

▨ Process   ● Key Milestone

CHAPTER 4
RESULTS AND DISCUSSION

4.1 PDC Single Cutter Test

4.1.1   PDC Single Cutter Analytical Model

The single cutter analytical model as shown in Figure 4.1 is used to study the cutter rock interaction. The cylinder represents the PDC cutter and the rectangle represents the granite formation. F_N and F_H is the normal force and the horizontal force applied on the cutter in the drilling process respectively. F_N is equal to the WOB applied on a single cutter. Depth of cut is equal to half of the cutter diameter. The cutter is moving at a constant velocity of 0.306 m/s. The two main parameters in this model are the back rake angle and the shape of cutter. PDC cutter with different back rake angle is used to drill the granite formation in Phase I. In Phase II, different shape of PDC cutter is used to drill the granite formation.

F_N

F_H PDC Cutter   V

Granite
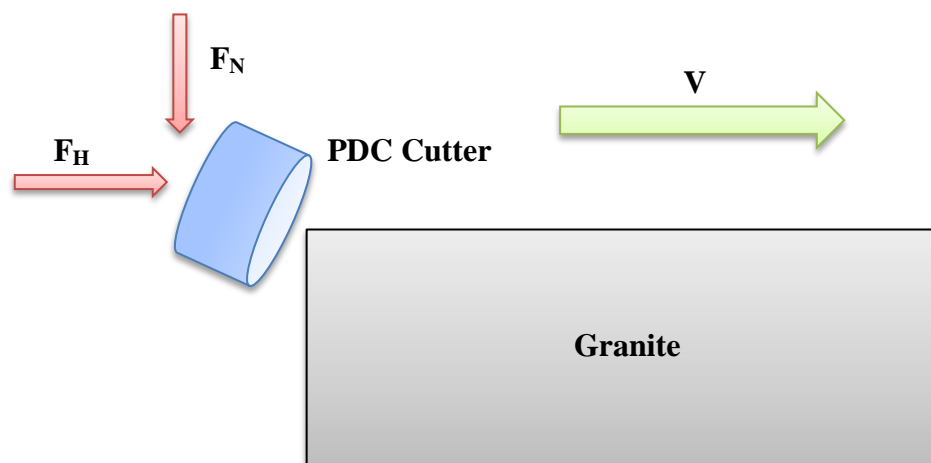
FIGURE 4.1 Single Cutter Model

4.1.1.1 Back Rake Angle

The data available for PDC cutter test with various back rake angle is shown in Table 4.1:

TABLE 4.1 Single Cutter Test Phase I Data

Parameter	*Value*
Normal Force, F_N	2500 N
Coefficient of Kinetic Friction, μ	0.45
Shape of the Cutter	Flat
Surface Area of Cutting Face, A	2.0106×10^{-4} m^2
Shear Contact Area, A_S	1.0053×10^{-4} m^2

To compute the horizontal force, the equation used is (Rajabov, et al., 2012):

$$F_H = F_N \left[\frac{1 - \mu \tan \alpha}{\tan \alpha + \mu} \right]$$

The relationship between the cutter back rake angles on the horizontal force is calculated and shown in Table 4.2.

TABLE 4.2 Horizontal Forces for Different Back Rake Angle

Back Rake Angle , α	**Horizontal Force, F_H (N)**
0˚	5555.56
5˚	4468.14
10˚	3674.81
15˚	3062.27
20˚	2568.32
30˚	1801.22

The data are used to plot the graph of horizontal force against back rake angle as shown in Figure 4.2 to study the effect of back rake angle on horizontal (shear) force.
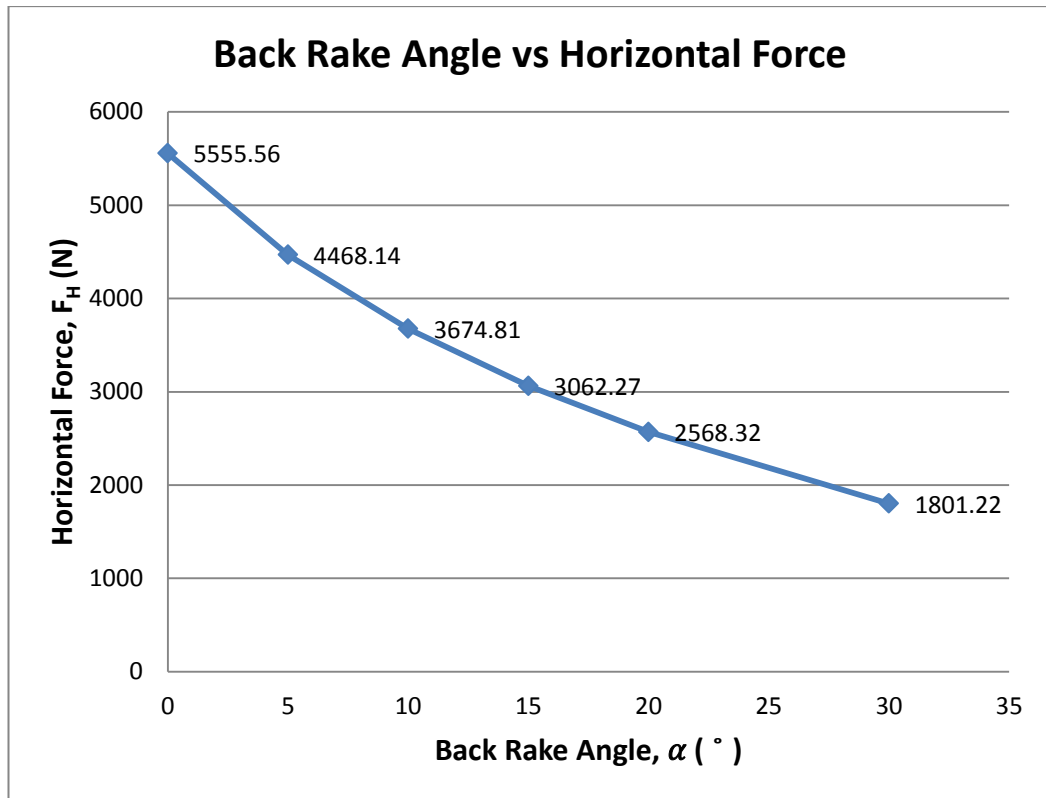
FIGURE 4.2 Graph of Horizontal Force vs Back Rake Angle

Result shows that cutter with higher back rake angle requires less horizontal force applied to cut the formation under a constant normal force.

Since the normal force applied on PDC cutter, size of the cutter and the depth of cut are constant, the axial stress is assumed the same for every cutter. By referring to Merchant's model, the normal stress on the cutter can be calculated by using the following equation:

$$\sigma = \frac{\text{Normal Frictional Force}}{\text{Contact Area}} = \frac{F_N}{A_N}$$

$$= \frac{2500N}{\pi(0.008m)(0.0185m)}$$

$$= 5.377 \text{ MPa}$$

The axial stress on the cutter is 5.377 MPa.

In drilling, the horizontal force is equivalent to the shear force. Thus, the horizontal force applied on each cutter is used to calculate the analytical shear stress as well as

to define the boundary condition of the simulation. By referring to Merchant's model, the shear stress on the cutter can be calculated by using the following equation:

$$\tau = \frac{\text{Horizontal Force}}{\text{Shear Contact Area}} = \frac{F_H}{A_S}$$

The axial stress and shear stress is totaled up to get the combined stress. The result for the shear stress for different back rake angled cutter is shown in Table 4.3.

TABLE 4.3 Calculated Stresses for Different Back Rake Angle

Back Rake Angle , α	Shear Stress, τ (MPa)	Combined Stress (MPa)
0˚	55.263	60.640
5˚	44.446	49.823
10˚	36.554	41.931
15˚	30.461	35.838
20˚	25.548	30.925
30˚	17.917	23.294

A graph of shear stress against back rake angle is plotted as shown in Figure 4.3 to study the effect on back rake angle on shear stress.
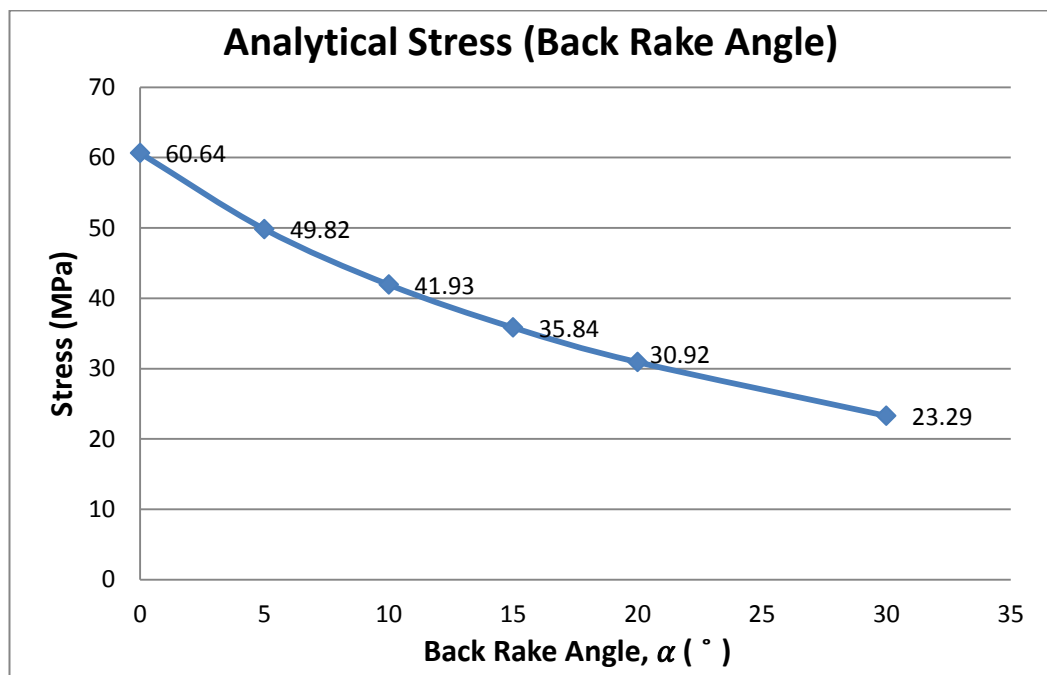
FIGURE 4.3 Effect of Back Rake Angle on Stress (Analytical)

35

The result shows that the cutter with higher back rake angle experiences less stress. This is because the horizontal force applied on the cutter decreases with the increased back rake angle, thus resulting in a lower shear stress.

The relationship between shear stress and horizontal force is shown in Figure 4.4.
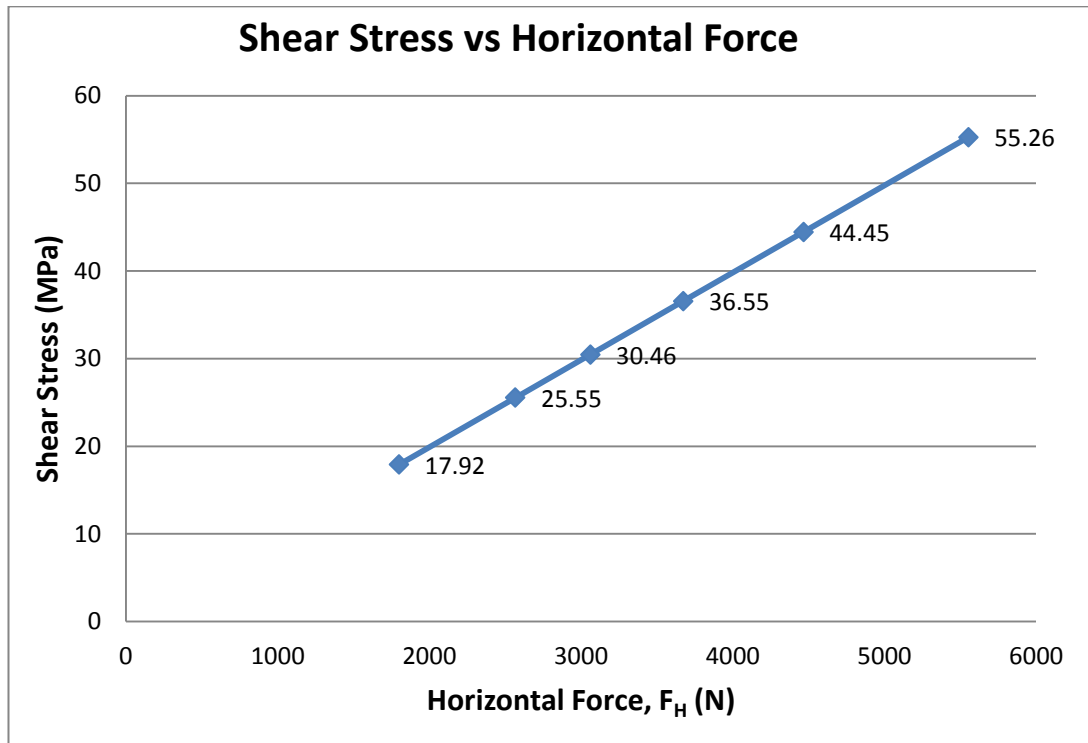
FIGURE 4.4 Graph of Shear Stress vs Horizontal Force (Analytical)

According to Figure 4.4, horizontal force is directly proportional to shear stress. Thus, lower back rake angle results in higher shear stress.

4.1.1.2 Shape of Cutter

Different shapes of PDC cutter are used to cut the granite formation with constant back rake angle. Since the cutter back rake angle is constant, thus the applied horizontal force is constant for all shapes of cutter. The shear contact area is taken to be half of the surface area of cutting face as the depth of cut is half of the cutter diameter. The data available for Phase 2 is shown in Table 4.4 and Table 4.5.

TABLE 4.4 Single Cutter Phase II Data

Parameter	*Value*
Normal Force, F_N	2500 N
Horizontal Force, F_H	2568.32 N
Coefficient of kinetic friction, μ	0.45
Back Rake Angle, α	20˚

TABLE 4.5 Shear Contact Areas of Different Shape of Cutter

Shape of Cutter	Surface Area of Cutting Face (m^2)	Shear Contact Area (m^2)
Beveled	3.1163×10^{-4}	1.5582×10^{-4}
Conical	3.0790×10^{-4}	1.5395×10^{-4}
Multidimensional	2.7705×10^{-4}	1.3853×10^{-4}
Flat	2.0106×10^{-4}	1.0053×10^{-4}

From Figure 4.5, we can see that beveled shaped cutter has the largest shear contact area, followed by conical, multidimensional and flat shaped cutter.

Shear Contact Area of PDC Cutter
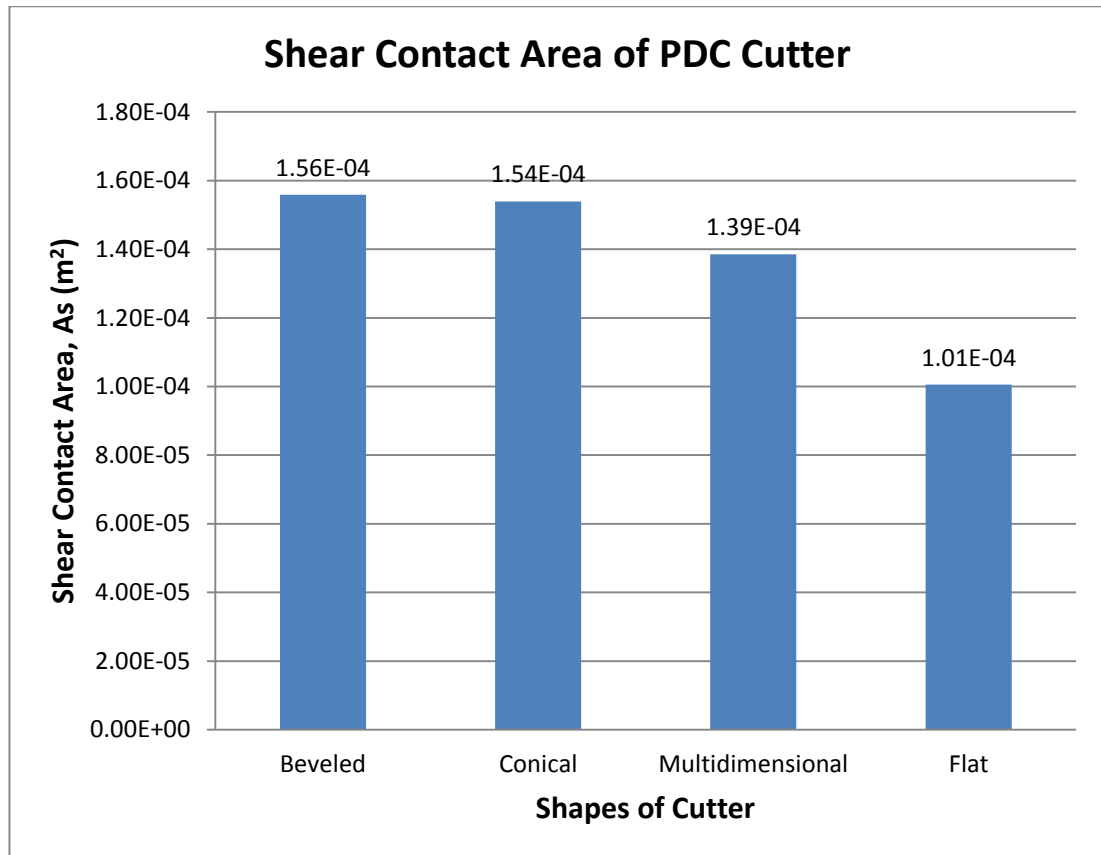
FIGURE 4.5 Shear Contact Areas for Different Shape of Cutter

The shear stress and axial stress is calculated using the formula of Merchant's model. The axial stress is taken as a constant for every cutter, with a value of 5.377 MPa. The result of the calculated stress for different shape of cutter is shown in the Table 4.6.

TABLE 4.6 Calculated Stresses for Different Shape of Cutter

Shape of Cutter	Shear Stress (MPa)	Combined Stress (MPa)
Beveled	16.483	21.859
Conical	16.683	22.060
Multidimensional	18.540	23.917
Flat	25.548	30.925

The shear stress for different shape of cutter is shown in Figure 4.6.

Analytical Stress (Shape of Cutter)

Shape of Cutter	Stress (MPa)
Beveled	21.859
Conical	22.060
Multidimensional	23.917
Flat	30.925

FIGURE 4.6 Stresses for Different Shape of Cutter (Analytical)

According to the figure, we can see that the beveled-shaped cutter has the lowest stress. This is because shear stress exerted on the cutter decreases with the increasing shear contact area.

4.1.2　PDC Single Cutter Simulation

The simulation is run by applying the horizontal force and normal force. The horizontal force applied on the cutter is the value obtained from the analytical model. The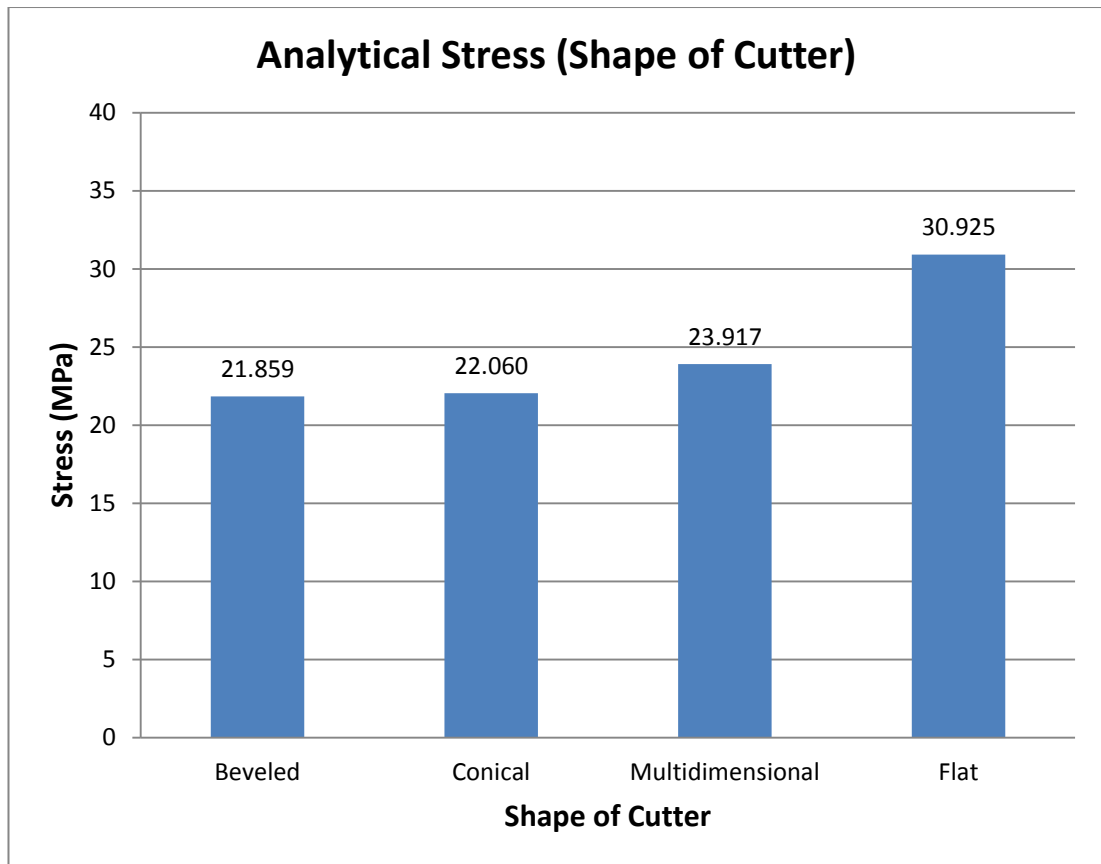 cutter shears the formation at a constant velocity of 0.306 m/s and the simulation period is set to be 60s in order to achieve a constant shearing force.

4.1.2.1 Back Rake Angle

Von Mises stress induced in the cutter with different back rake angle is tabulated in Table 4.7.

TABLE 4.7　Simulation Data for Different Back Rake Angle

Time (s)	Back Rake Angle					
	0°	5°	10°	15°	20°	30°
	Stress (Pa)					
0.0	0	0	0	0	0	0
2.5	1.45E+07	1.18E+07	9.80E+06	8.81E+06	8.14E+06	7.51E+06
5.0	3.24E+07	2.86E+07	2.42E+07	2.18E+07	1.95E+07	1.70E+07
7.5	4.93E+07	4.58E+07	3.81E+07	3.55E+07	2.99E+07	2.62E+07
10.0	6.50E+07	6.14E+07	4.92E+07	4.75E+07	3.86E+07	3.26E+07
12.5	8.15E+07	7.25E+07	6.06E+07	5.44E+07	4.47E+07	3.70E+07
15.0	8.53E+07	7.18E+07	6.09E+07	5.32E+07	4.81E+07	3.88E+07
17.5	8.41E+07	6.82E+07	5.88E+07	5.07E+07	4.70E+07	3.70E+07
20.0	8.25E+07	6.76E+07	5.57E+07	4.95E+07	4.42E+07	3.48E+07
22.5	8.08E+07	6.79E+07	5.54E+07	4.87E+07	4.34E+07	3.40E+07
25.0	7.90E+07	6.75E+07	5.64E+07	4.95E+07	4.29E+07	3.35E+07
27.5	7.91E+07	6.65E+07	5.79E+07	5.15E+07	4.27E+07	3.27E+07
30.0	7.92E+07	6.72E+07	5.70E+07	4.95E+07	4.16E+07	3.30E+07
32.5	7.94E+07	6.62E+07	5.77E+07	5.02E+07	4.31E+07	3.41E+07
35.0	7.87E+07	6.81E+07	5.81E+07	4.99E+07	4.24E+07	3.19E+07
37.5	7.95E+07	6.59E+07	5.78E+07	4.85E+07	4.32E+07	3.21E+07
40.0	7.87E+07	6.61E+07	5.74E+07	4.75E+07	4.19E+07	3.23E+07
42.5	7.96E+07	6.60E+07	5.62E+07	4.83E+07	4.35E+07	3.15E+07

45.0	8.00E+07	6.78E+07	5.59E+07	4.79E+07	4.21E+07	3.23E+07
47.5	7.92E+07	6.61E+07	5.65E+07	4.93E+07	4.18E+07	3.32E+07
50.0	7.87E+07	6.55E+07	5.73E+07	4.83E+07	4.23E+07	3.41E+07
52.5	7.97E+07	6.60E+07	5.59E+07	4.80E+07	4.22E+07	3.37E+07
55.0	7.93E+07	6.58E+07	5.67E+07	4.78E+07	4.27E+07	3.29E+07
57.5	7.90E+07	6.60E+07	5.60E+07	4.82E+07	4.31E+07	3.34E+07
60.0	7.98E+07	6.59E+07	5.59E+07	4.76E+07	4.25E+07	3.28E+07

A graph of stress against time for different back rake angle is plotted in Figure 4.7.
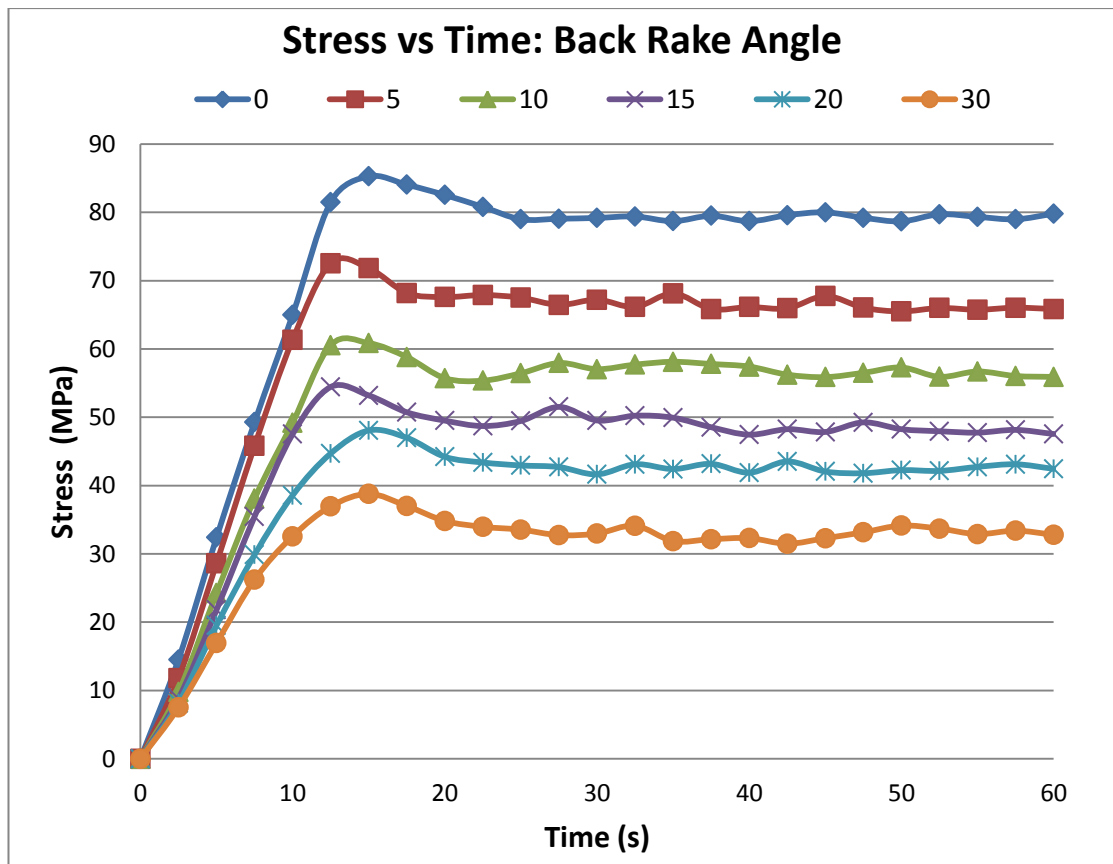

FIGURE 4.7 Graph of Stress vs Time for Different Back Rake Angle

The stress on the cutter is increasing at the beginning of the simulation. This is because the horizontal force is increased in amplitude and started to reach the applied horizontal force value only after a certain period. In order to ensure the accuracy of the result, the average stress is only taken after a period of 10s.

The average von Mises stress induced in each PDC cutter with different back rake angle is tabulated in Table 4.8 below respectively.

TABLE 4.8 Average Stresses for Different Back Rake Angle

Back Rake Angle , α	Average Stress (MPa)
0˚	80.15
5˚	67.22
10˚	57.22
15˚	49.42
20˚	43.27
30˚	33.76

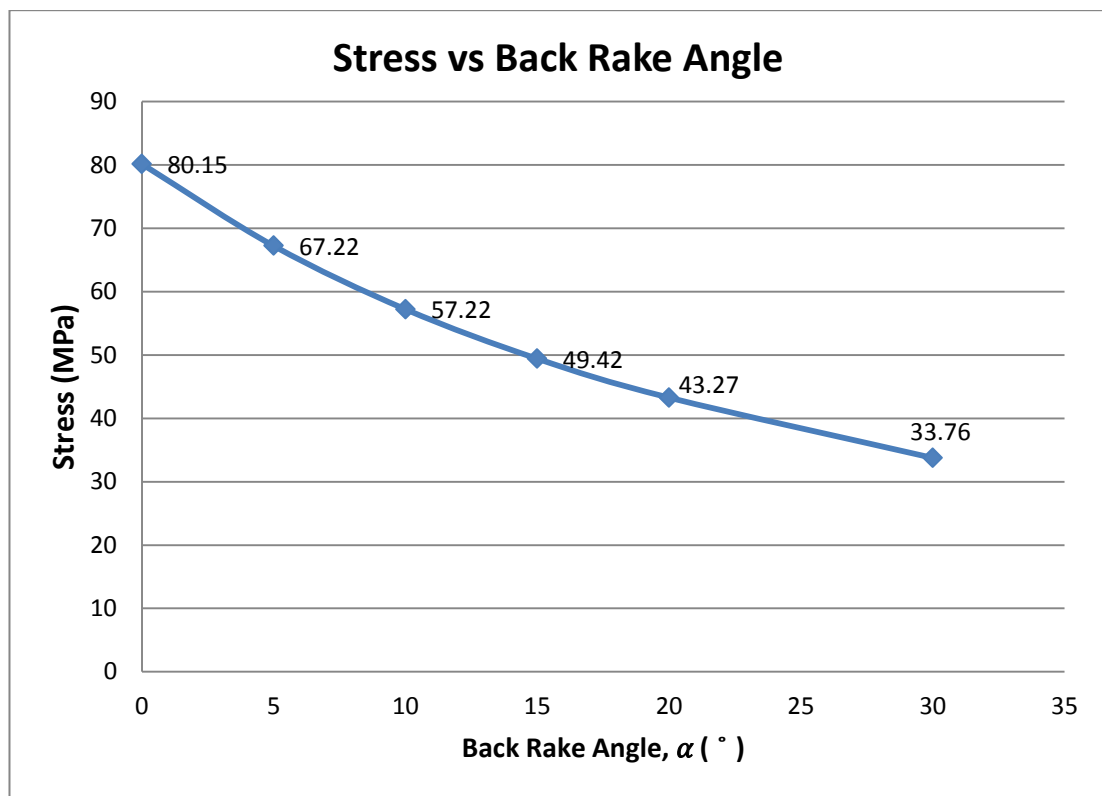Figure 4.8 is plotted to study the relationship of back rake angle and stress.

FIGURE 4.8 Effects on Back Rake Angle on Stress (Simulation)

Result shows that higher back rake angle has lower von Mises stress induced in the cutter. This is due to the lower horizontal force applied on the cutter. A graph of simulated stress vs horizontal force as shown in Figure 4.9 is plotted to analyse the

interaction between these two variables. Stress is found to be proportional to the applied horizontal force. Cutter with back rake angle of $30°$ has the lowest horizontal force applied under a constant normal force. Thus, the stress induced in the $30°$ back rake angled cutter is the lowest.

Horizontal Force vs Stress

Stress (MPa) vs Horizontal Force, F_N (N)

- 33.76
- 43.27
- 49.42
- 57.22
- 67.22
- 80.15
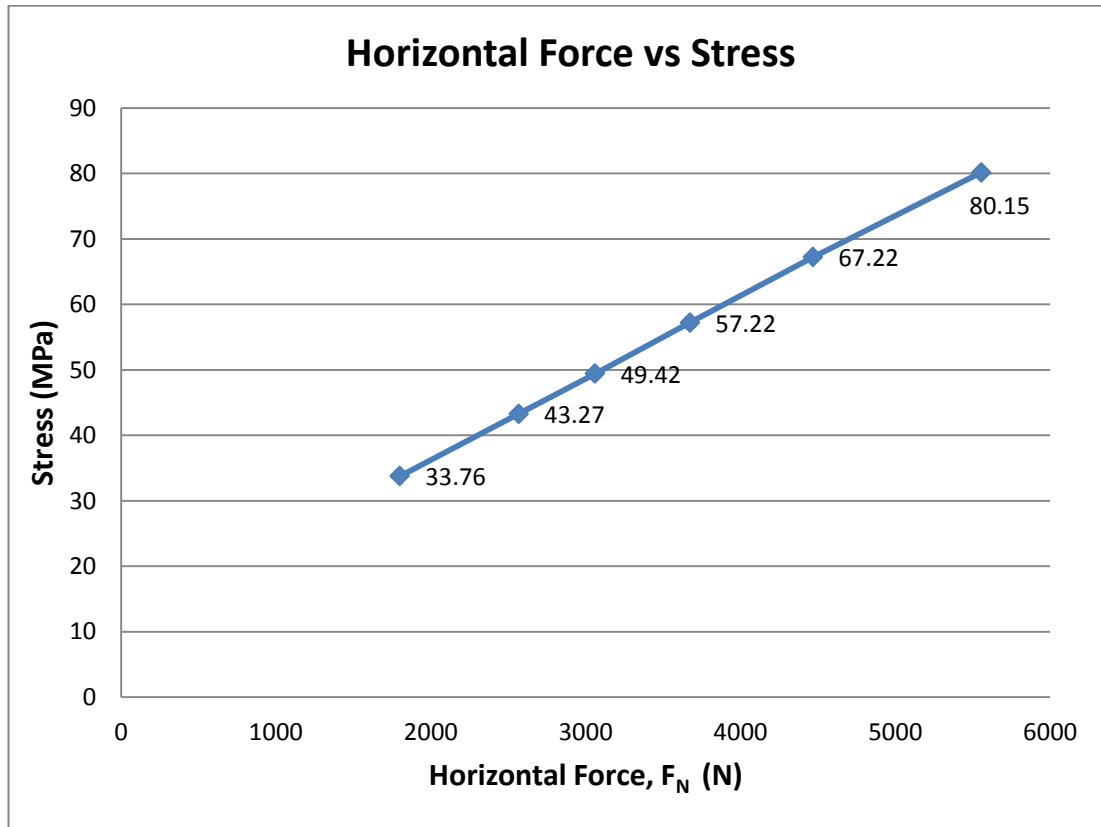
FIGURE 4.9 Graph of Stress vs Horizontal Force (Simulation)

A comparative analysis of the simulation result and analytical result of different back rake angled cutter is shown in Table 4.9.

TABLE 4.9   Stress Values for Different Back Rake Angle

Back Rake Angle , α	Simulated Stress (MPa)	Analytical Stress (MPa)
$0°$	80.15	60.64
$5°$	67.22	49.82
$10°$	57.22	41.93
$15°$	49.42	35.84
$20°$	43.27	30.93
$30°$	33.76	23.29

The comparison between analytical stress and simulated stress is shown in Figure 4.10.
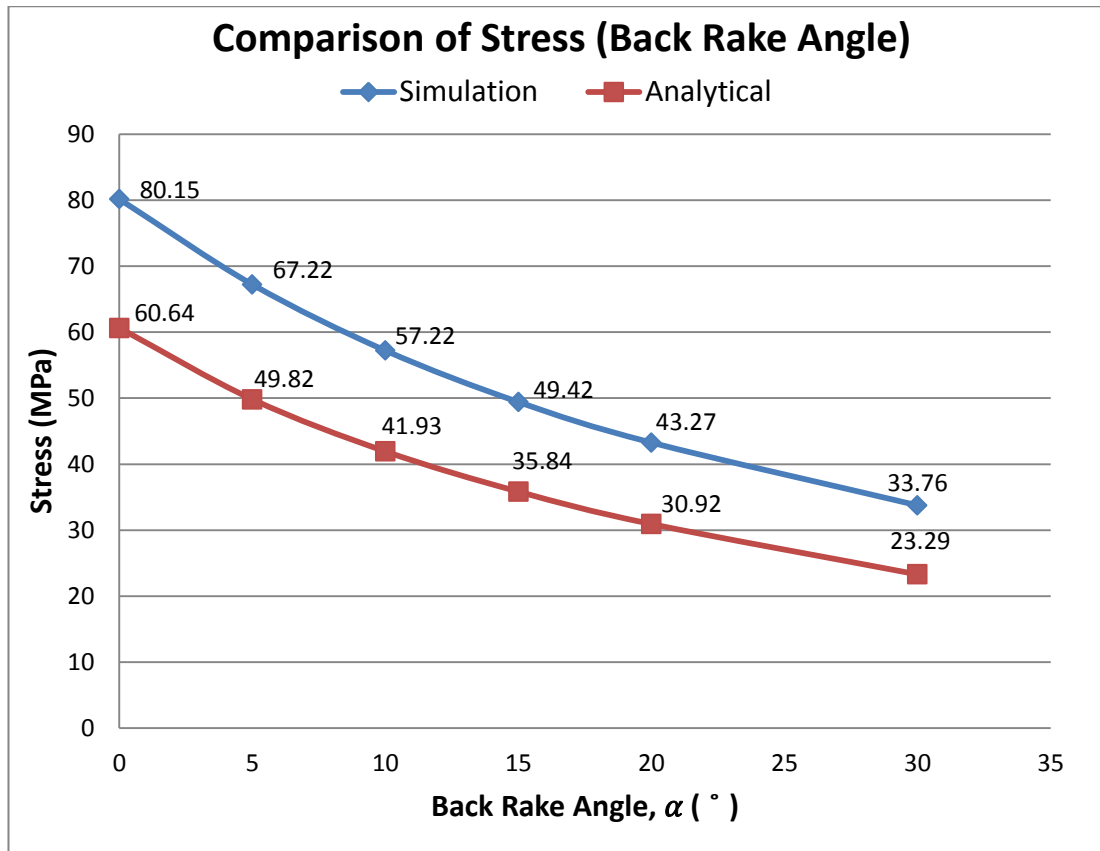
FIGURE 4.10 Comparison of Stresses for Different Back Rake Angles

The stress obtained from the simulation is found to be higher than analytical result. The highest percentage of difference for the result is approximately 27.22%. This may be due to the hydrostatic stress exerted on the cutter. Besides, the normal contact area may be smaller which results in a higher normal force. The mesh sizes of the model also influence the result. At the same time, combined with analytical result, with the increase of back rake angle, the stress value is decreased, verifying the correctness of the simulation result. PDC cutter with 30˚ back rake angle has proved to have the lowest stress values.

4.1.2.2 Shape of Cutter

Von Mises stress induced in the different shapes of cutter is tabulated in Table 4.10.

TABLE 4.10 Simulation Data for Different Shape of Cutter

Time (s)	Shapes of Cutter			
	Beveled	Conical	Multidimensional	Flat
	Stress (Pa)			
0.0	0	0	0	0
2.5	2.01E+06	3.77E+06	3.18E+06	8.14E+06
5.0	3.56E+06	6.02E+06	6.74E+06	1.95E+07
7.5	5.29E+06	8.40E+06	1.09E+07	2.99E+07
10.0	7.30E+06	1.05E+07	1.53E+07	3.86E+07
12.5	9.81E+06	1.35E+07	1.92E+07	4.47E+07
15.0	1.29E+07	1.70E+07	2.35E+07	4.81E+07
17.5	1.60E+07	1.80E+07	2.64E+07	4.70E+07
20.0	1.85E+07	1.89E+07	2.83E+07	4.42E+07
22.5	2.15E+07	1.97E+07	2.81E+07	4.34E+07
25.0	2.36E+07	2.08E+07	2.91E+07	4.29E+07
27.5	2.46E+07	2.30E+07	3.15E+07	4.27E+07
30.0	2.40E+07	2.56E+07	3.22E+07	4.16E+07
32.5	2.45E+07	2.64E+07	3.12E+07	4.31E+07
35.0	2.42E+07	2.76E+07	3.16E+07	4.24E+07
37.5	2.36E+07	2.84E+07	3.12E+07	4.32E+07
40.0	2.29E+07	2.75E+07	3.06E+07	4.19E+07
42.5	2.32E+07	2.74E+07	3.04E+07	4.35E+07
45.0	2.37E+07	2.69E+07	3.05E+07	4.21E+07
47.5	2.37E+07	2.74E+07	3.12E+07	4.18E+07
50.0	2.34E+07	2.78E+07	3.14E+07	4.23E+07
52.5	2.29E+07	2.77E+07	3.21E+07	4.22E+07
55.0	2.35E+07	2.70E+07	3.12E+07	4.27E+07
57.5	2.40E+07	2.72E+07	3.15E+07	4.31E+07
60.0	2.37E+07	2.72E+07	3.11E+07	4.25E+07

A graph of stress against time for different shape of cutter is plotted in Figure 4.11.
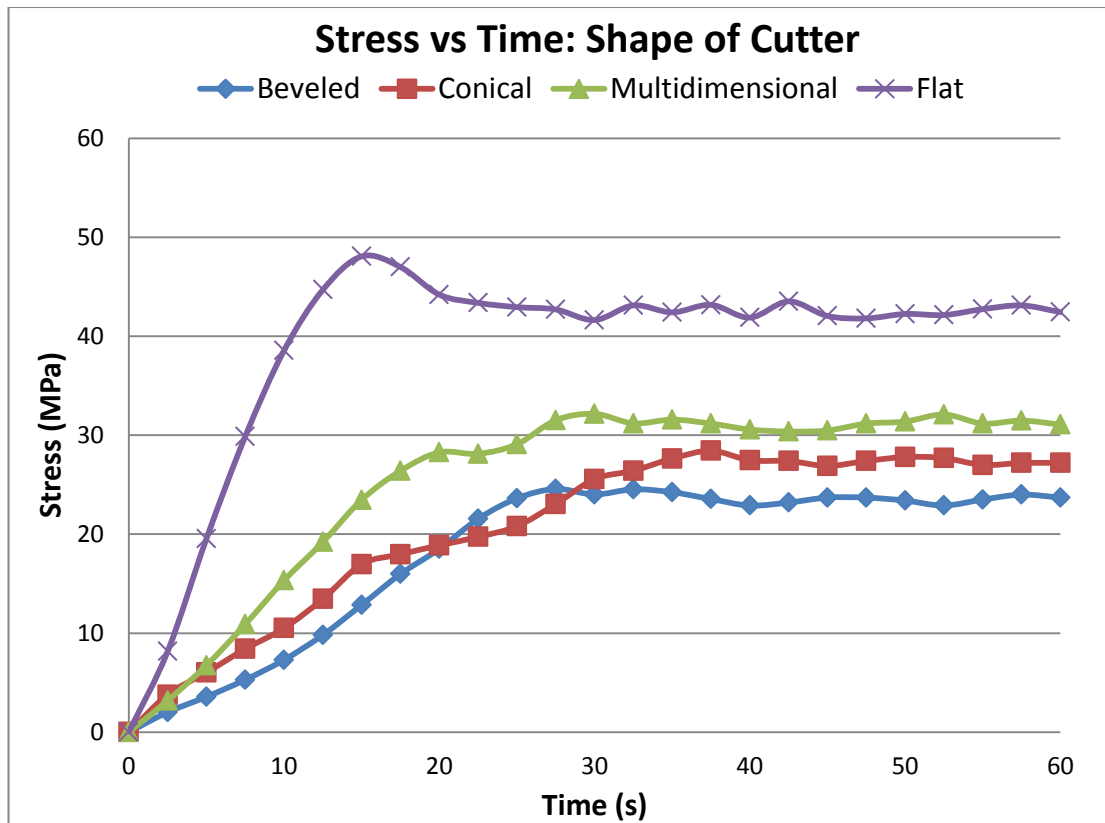
FIGURE 4.11 Graph of Stress vs Time for Different Shape of Cutter

The stress induced in the cutter increases at the beginning of the simulation and becomes stable after a period of time. The cutters with non-flat diamond table like conical and multidimensional require longer time to achieve a consistent stress value. In order to ensure the accuracy of the result, the average stress is calculated once the stress value becomes stable.

The average von Mises stress for PDC cutter with different shape is tabulated in Table 4.11 below.

TABLE 4.11 Average Stresses for Different Shapes of Cutter

Shape of Cutter	Average Stress (MPa)
Beveled	23.71
Conical	27.24
Multidimensional	31.25
Flat	43.27

Figure 4.12 is plotted to show the average von Mises stress induced in each PDC cutter with different shape.
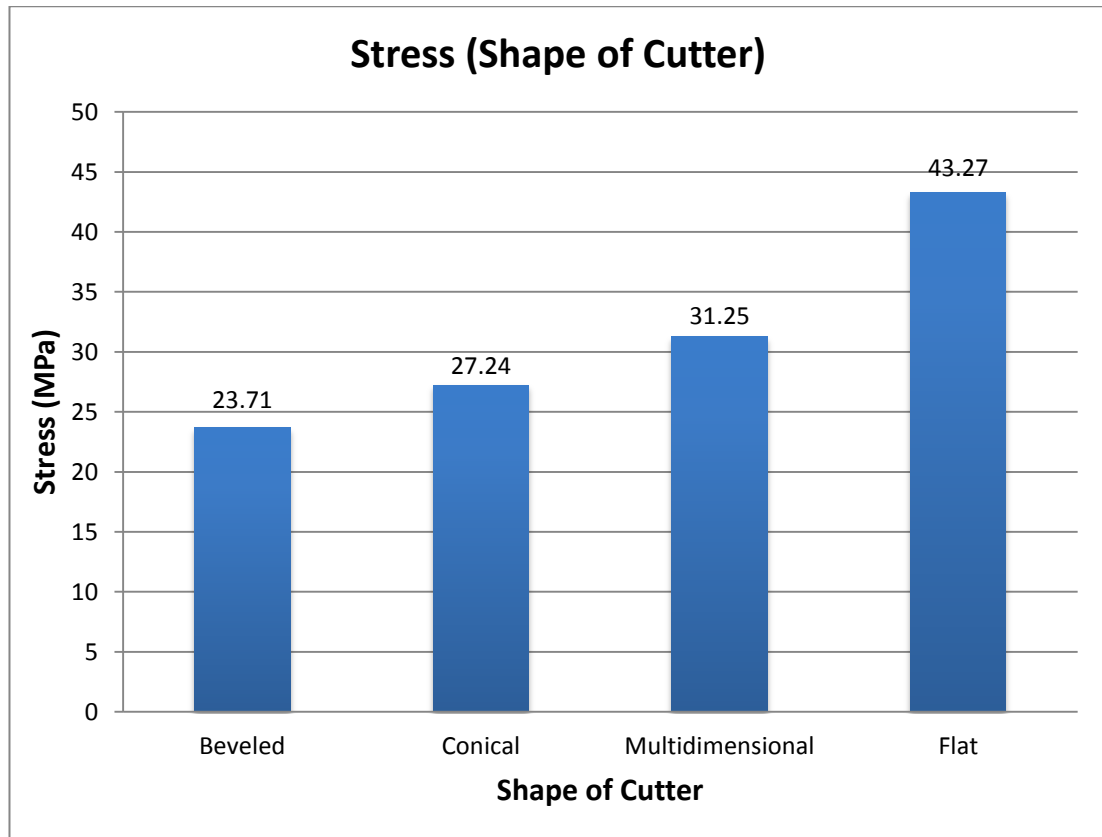
FIGURE 4.12 Stresses for Different Shape of Cutter (Simulation)

Based on the figure, we can see that beveled-shaped cutter has the lowest von Mises stress, followed by conical, multidimensional and flat-shaped cutter. This is because stress is depended on the shear surface area. Increased shear contact area reduces the stress exerted on the cutter.

The simulation result is compared the analytical result as shown in Table 4.12.

TABLE 4.12 Stress Values for Different Shape of Cutter

Shape of Cutter	Simulated Stress (MPa)	Analytical Stress (MPa)
Beveled	23.71	21.86
Conical	27.24	22.06
Multidimensional	31.25	23.92
Flat	43.27	30.92

The comparison between analytical stress and simulated stress for different shapes of cutter is shown in Figure 4.13.
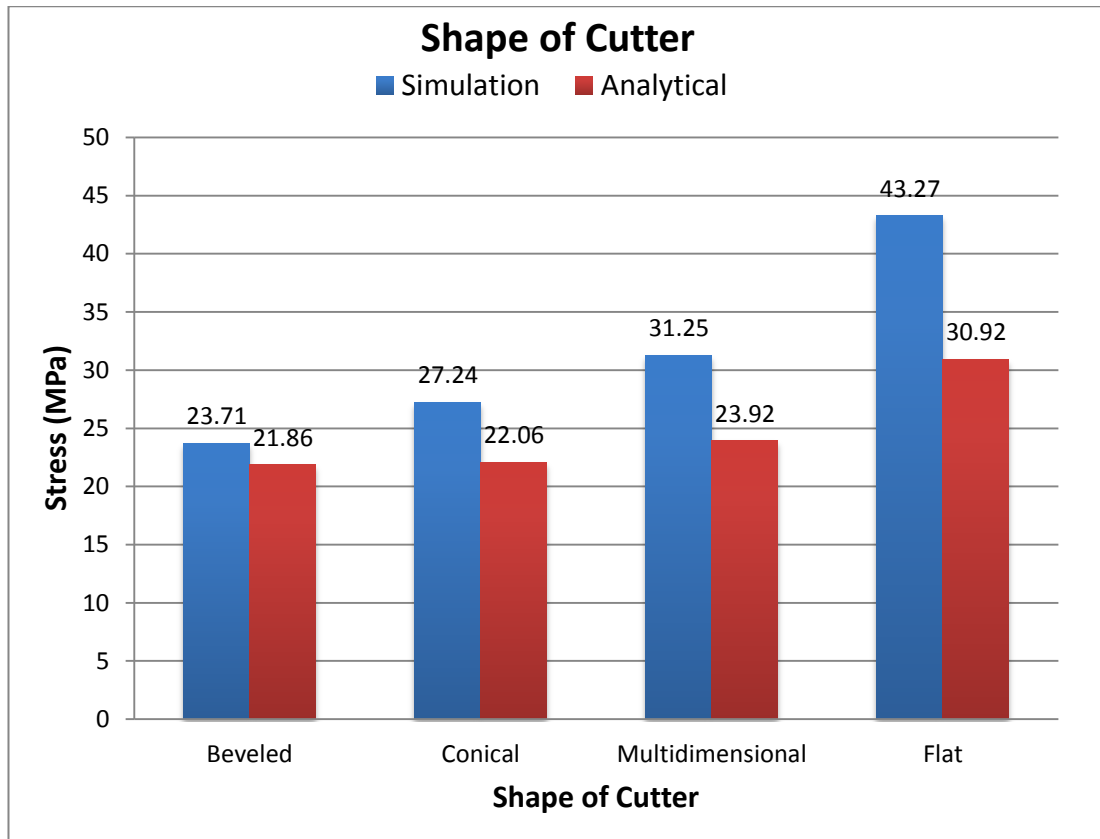
FIGURE 4.13 Comparison of Stresses for Different Shape of Cutter

The stress obtained from the simulation is generally higher than analytical result. The highest percentage of difference for the result is approximately 33.29 %. This is most probably due to and hydrostatic stress induced in the cutter. Besides, the normal contact area may be smaller which results in a higher normal force. Furthermore, the inconsistence cutter face may result in higher contact force which results in higher stress. The result is also dependent on the mesh sizes of the cutter model. Beveled-shaped cutter has the lowest stress value for both analytical and simulation result.

4.2   PDC Cutter Wear Rate

After the analysis of PDC cutter in the process of drilling and the stress distribution is put into the solving theory of cutter wear rate to analyse wear. The wear per sliding distance of the PDC cutter is calculated using the equation (Tangena, 1988):

$$W = k_2 V \overline{\sigma}^{\frac{1}{bn'}}$$

Parameters Used:

Proportionality constant, $k_2 \times V = 1.5 \times 10^{-11}$

$\frac{1}{bn'} = 6.45$

k_2 is an arbitrary wear constant, V is the deformed volume, $\overline{\sigma}$ is the von Mises stress in MPa, b is a constant whose value is approximately 0.5, and n' is the cyclic strain-hardening coefficient. Volume of deformed material, V, is approximately equal to Π x a^2 x d, where a is the contact radius and d the thickness of the layer. For simplicity, the volume of deformed material V is taken as constant compared to the von Mises stress to the power of 6.45 to construct the wear model.

The stress values are taken from both simulation and analytical model. From the equation, the higher stress values will result in higher wear if other parameters are kept constant. The magnitude of the stress is dependent on the contact geometry, the mechanical properties of the materials, the friction and the externally applied forces. In this study, the mechanical properties of the materials and rock friction are kept constant. A correct cutters repartition on the bit is assumed, which ensures a homogenized wear on every PDC Therefore, wear behaviour based on single cutter experiments are relevant and can be extrapolated to understand the whole bit behaviour.

4.2.1 Back Rake Angle

The wear of the different back rake angled cutter is shown in Table 4.13.

TABLE 4.13 Wear Values of PDC Cutter (Back Rake Angle)

Back Rake Angle , α	Simulated Stress (MPa)	Analytical Stress (MPa)	Simulated Wear (μm^2)	Analytical Wear (μm^2)
0˚	80.155	60.640	28.604	4.7301
5˚	67.223	49.823	9.195	1.3320
10˚	57.216	41.931	3.251	0.4380
15˚	49.416	35.838	1.263	0.1591
20˚	43.271	30.925	0.536	0.0615
30˚	33.758	23.294	0.182	0.0099

Since the simulation period is 60s, the wear rate of the cutter can be computed by dividing the cutter wear over the time. The wear rate of different back rake angled cutter is tabulated in Table 4.14.

TABLE 4.14 Wear Rates of PDC Cutter (Back Rake Angle)

Back Rake Angle , α	Simulated Wear Rate (μm^2/s)	Analytical Wear Rate (μm^2/s)
0˚	0.4767	0.0788
5˚	0.1533	0.0222
10˚	0.0542	0.0073
15˚	0.0211	0.0027
20˚	0.0089	0.0010
30˚	0.0018	0.0002

A graph of wear rate vs back rake angle as shown in Figure 4.14 is plotted to analyse the relationship between back rake angle and cutter wear rate.
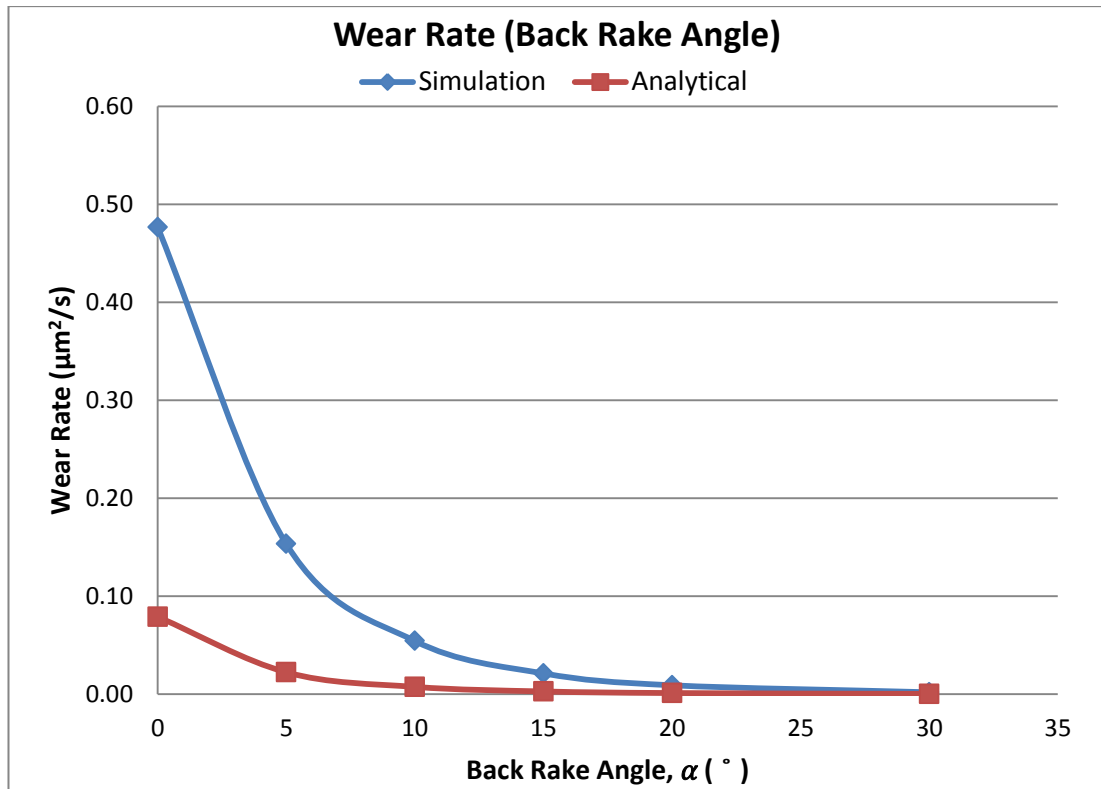
FIGURE 4.14 Graph of Wear Rate vs Back Rake Angle

From the Figure 4.14, we can see that the cutter wear rate decreases as the back rake angle increases, but the decreasing trend is nonlinear. As mentioned, externally applied force affects the magnitude of stress. Keeping the other operational parameters constant, higher cutter back rake angle requires less horizontal force applied to cut the formation at a constant normal force. The horizontal force reduces three-fold when the back rake angle increases 10˚ to 30˚ under the same cutting area. Thus, PDC cutter with 30˚ back rake angle has the minimum stress value due to the lowest applied horizontal force.

The cutter fails once the von Mises stress induced in the cutter exceeds yield strength of the cutter. Thus, cutter wear rate is affected by the cutter back rake angle. With the increase of the back rake angle of the PDC cutter, the cutter wear rate decreases significantly. Thus, 30˚ back rake angle with the lowest stress is the best design to reduce wear rate in drilling granite formation. At the same time, combined with analytical result, with the increase of back rake angle, the cutter wear rate is decreased, verifying the correctness of the simulation result. However, cutter back rake angle higher than 45˚ should be avoided in drilling as very large back rake angled tool have less mechanical strength which reduces tool life.

4.2.2 Shape of Cutter

The wear value of each cutter with different shape is shown in the Table 4.15.

TABLE 4.15 Wear Values of PDC Cutter (Shape of Cutter)

Shape of Cutter	Simulated Stress (MPa)	Analytical Stress (MPa)	Simulated Wear (μm^2)	Analytical Wear (μm^2)
Beveled	23.708	21.859	0.0111	0.0066
Conical	27.241	22.060	0.0271	0.0070
Multidimensional	31.248	23.917	0.0657	0.0117
Flat	43.270	30.925	0.5365	0.0615

The cutter wear is divided by the simulation period of 60s to determine the wear rate. The wear rate of the each cutter with different shape is tabulated in Table 4.16.

TABLE 4.16 Wear Rates of PDC Cutter (Shape of Cutter)

Shape of Cutter	Simulated Wear Rate ($\mu m^2/s$)	Analytical Wear Rate ($\mu m^2/s$)
Beveled	0.00019	0.00011
Conical	0.00045	0.00012
Multidimensional	0.00110	0.00020
Flat	0.00894	0.00102

A graph of wear rate vs shape of cutter is plotted as shown in Figure 4.15 to analyse the relationship between shape of cutter and cutter wear rate.
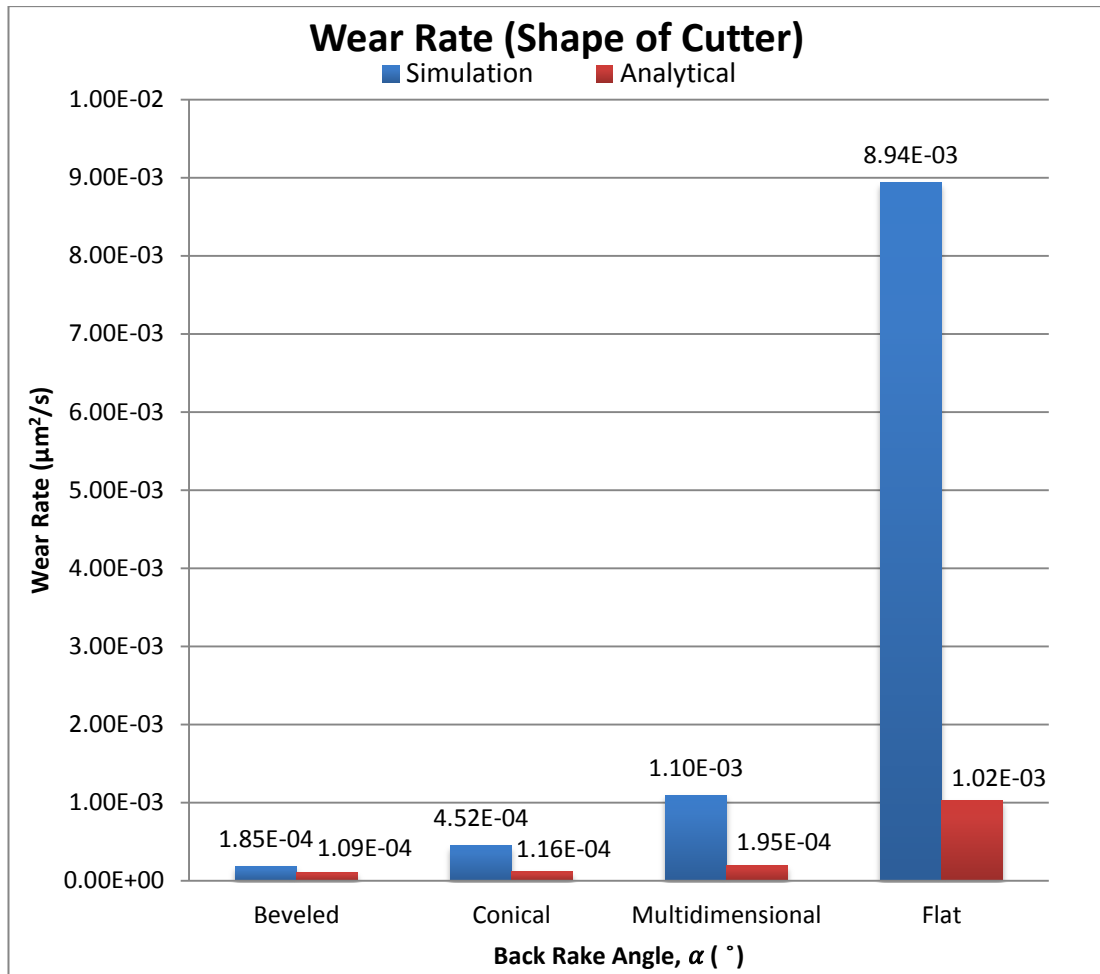
Wear Rate (Shape of Cutter)

FIGURE 4.15   Graph of Wear Rate vs Shape of Cutter

Result shows beveled-shaped cutter has the lowest wear rate of 1.85×10^{-4} μm^2/s. The shape of PDC cutter has a great effect on the cutting area. This is because different shape of PDC cutter is having different contact geometry that affects the amount of stress induced under a constant back rake angle. The cutter will fail once the von Mises stress induced in the cutter exceeds yield strength of the cutter. So, shear contract area of cutter should be maximized to enhance the cutter life.

Beveled-shaped cutter with the largest shear contact area of 1.56×10^{-4} m^2 is having the largest contact geometry. Increased cutter geometry helps to reduce the stress induced in the cutter. At the same time, combined with analytical result, with the increase of contact geometry, the cutter wear rate is decreased, verifying the correctness of the simulation result. Thus, beveled-shaped cutter with the largest cutter geometry is the most suitable design for drilling hard formation in order to minimize the cutter wear rate.

CHAPTER 5
CONCLUSION AND RECOMMENDATION

5.1 Conclusion

This project reported the result of rock cutting tests performed with PDC cutters at various back side rake angles and with various shapes. All the objectives of the project are achieved. A single cutter analytical model is used to study the forces and stress in each PDC cutter in removing granite formation. The model combined the cutter-rock interaction model and Merchant's cutting model for analysis. Result indicated that back rake angle and shape of cutter have significant effects on stress distribution. Application of the model for simulation test showed that higher horizontal force and larger contact geometry reduce the stress indicated on cutter. Effect of back rake angle and shape of PDC cutter on the rule of cutting element wear are analyzed by using the wear theory. Higher back rake angle has less applied horizontal force, thus resulting in lower shear stress and this helps to reduce cutter wear rate. Shear stress indicated in the cutter with larger contact area is smaller, thus lowering the cutter wear rate. In a conclusion, 30˚ back rake angled cutter and beveled-shaped cutter are found to be the best design to reduce cutter wear rate in hard formation.

5.2 Recommendation

Lab test is recommended to be carried out in the future to further verify the result. In order to improve the accuracy of the result, wear model for PDC cutter should be developed based on the field data. Full PDC bit analysis is not able to be carried out in this project due to the limitations of the software license. Thus, fully licensed software is recommended to increase the accuracy of the result in the future. Other design parameters should be included to optimize the PDC bit design for hard formation application. Both ROP and bit durability should be analysed together to optimize the PDC bit for drilling faster and further in hard formation.

REFERENCES

Bilgesu, H.I., Tetrick, L.T., Altmis, U., Mohaghegh, S., and Ameri, S., (1997). "A New Approach for the Prediction of Rate of Penetration (ROP) Values" *SPE Journal*.

Bit Technology, (2012). Baker Hughes Incorporated.

Che, D., Han, P., Guo, P., and Ehmann, K., (2012). "Issues in Polycrystalline Diamond Compact Cutter-Rock Interaction From a Metal Machining Point of View Part I: Temperature, Stresses, and Forces" *Journal of Manufacturing Science and Engineering*, **134**.

Cheatham, C.A. and Loeb, D.A., (1985). "Effect of Field Wear on PDC Bit Performance" *SPE/IADC Journal*.

Clayton, R., Chen, S., and Lefort, G., (2005). "New Bit Design, Cutter Technology Extend PDC Applications to Hard Rock Drilling" *SPE Journal*.

Drilling Engineering Workbook, (1995). Baker Hughes INTEQ.

IADC Dull Grading System for Fixed Cutter Bits and Roller Cone Bits, (2012). Baker Hughes Incorporated.

Fear, M.J., (1999). "How to Improve Rate of Penetration in Field Operations" SPE Journal **14 (1)**.

Forbes, I. G. (July, 2012). *Operating Parameters – PDC Bits. Knect Baker Hughes Knowledge Management*. Retrieved June 15, 2014, from https://programs.bakerhughes.com/KMTools/iKnow/Pages/Operating%20Parameters%20-%20PDC%20Bits.aspx

Gao, F.Q., H, A.J., and Yang, X.L., (2010). "Numerical Analysis of Dynamic Mechanical Properties for Rock Sample under Strong Impact Loading" *International Journal Information Engineering and Electronic Business* **2**, 10-16.

Glowka, D. A., (1987). *Development of a Method for Predicting the Performance and Wear of PDC Drill Bits*. Report SAND86-1745, Sandia Natl. Laboratories, New Mexico, UCS.

Glowka, D.A. and Stone, C.M., (1986). "Effects of Thermal and Mechanical Loading on PDC Bit Life" *SPE Journal*.

Hareland, G., Yan, W., Nygaard, R., and Wise, J.L., (June, 2009). "Cutting Efficiency of aSingle PDC Cutter on Hard Rock" *Journal of Canadian Petroleum Technology*, **48 (6)**.

Hareland, G. and Rampersad, P. R., (1994). "Drag-Bit Model Including Wear" *SPE Journal*.

Henry, T., Corp, A., Sherif, M. and Ahmed Ragheb, (2011). "New PDC Technologies Increases Durability and Enables Fast Drilling in Hard Abrasive Formation" *SPE Jornal*.

Hussein A., Al-Anezi, N.A., Al-Sarraf, A.Q., Dhabria, A.K., Baqer, H. A., Maliekkal, H., Ghoneim, O., Zhang,Y.,2013. "Thermally Stable Cutter Technology Advances PDC Performance in Hard and Abrasive Formations, Kuwait" *SPE Journal.*

Juneja, B.L., Sekhon, G.S. and Seih,N., (2003). *Fundamentals of Metal Cutting and Machine Tool*, India: New Age International.

Kuru, E, Wojtanowicz, A.K., (1986). "A Method of Detecting In-Situ PDC Bit Dull and Lithology Change" *SPE Journal.*

Li, X.H. and Hood, M., (1993). "Wear and damage to PDC bits" *SPE Journal*.

Liu, Z., Marland, D. and Samuel, R., (2014). "An Analytical Model Coupled With Data Analytics to Estimate PDC Bit Wear" *SPE Journal*.

Maute, R. E., (2005). *Practical Interpretation of Open Hole Logs*. 2000-2500 RSE, Inc. Texas, USA.

Mohd Noor, M.H., (2014). *Optimizing PDC Bit Design Features for Improvement in Rate of Penetration for Multi-layer Formation*. Universiti Teknologi PETRONAS, Perak, Malaysia.

Motahhari, H.R., (2008). *Improved Drilling Efficiency Technique Using Integrated PDM and PDC Bit Parameters*. University of Calgary, Calgary, Alberta.

Rajabov, V., Miska, S., Mortimer, L., Yu, M., and Ozbayoglu, E., (2012). "The Effects of Back Rake and Side Rake Angles on Mechanical Specific Energy of Single PDC Cutters with Selected Rocks at Varying Depth of Cuts and Confining Pressures" *SPE Journal*.

Robertson, E.C, (1988). *Thermal Properties of Rocks*. Report Number 88-441, Department of the Interior Geological Survey, United States.

Schouwenaars, R., Jacobo, V.H., and Ortiz, A., (2009). "Transition from normal to severe wear in PCD during high-speed cutting of a ductile material" *International Journal of Refractory Metals and Hard Materials 27(2)*: 403 - 408.

Tangena, A.G., (1987). Tribology of thin film system, Doctoral thesis, indveran Technical University.

Tangena, A.G. and Wijnhoven, P.J.M., (1988). The correlation between mechanical stresses and wear in layered system, Wear, 121, 27-35.

Tian, J. L., Fu, C.H., Yang, L., Pang, X.L., Li, Y., Zhu, Y.H., and Liu, G., (2014). *The Wear Analysis Model of Drill Bit Cutting Element with Torsion Vibration.* School of Mechanical Engineering, Southwest Petroleum University, Chengdu, China.

Warren, T. M. and Sinor, A., (1986). "Drag Bit Performance Modeling" *SPE Journal*.

Wesrling, L, Lundberg, P. and Lundberg, B., (2001). "Tungsten long-rod penetration into confined cylinders of boron carbide at and above ordnance velocities" *International Journal of Impact Engineering* **25**: 703-714.

Wilmot, G.M. and Penrose, B., (2003). "Advanced Cutting Structure Improves PDC Bit Performance in Hard and the Drilling Environments" *SPE Journal*.

Yahiaoui, M., Gerbaud, L. Paris, J-Y., Denape, J., and Dourfaye, A., (2012). *A Study on PDC Drill Bits Quality.* Ecole Nationale d'Ingénieurs de Tarbes, Tarbes, France.
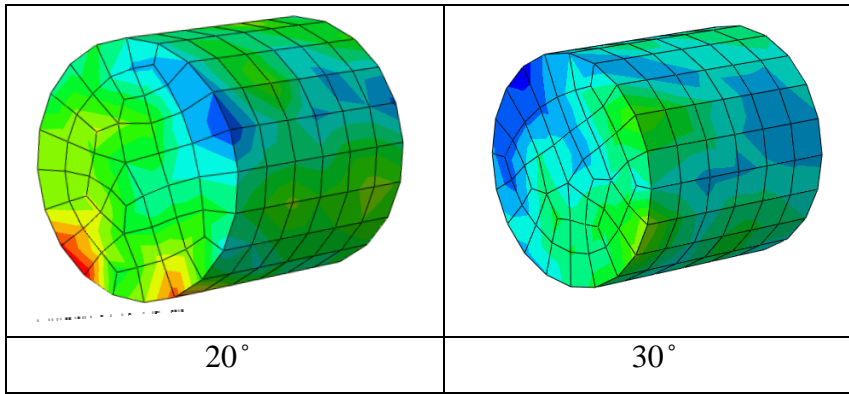
APPENDICES

APPENDIX 1.1 Single Cutter Simulation
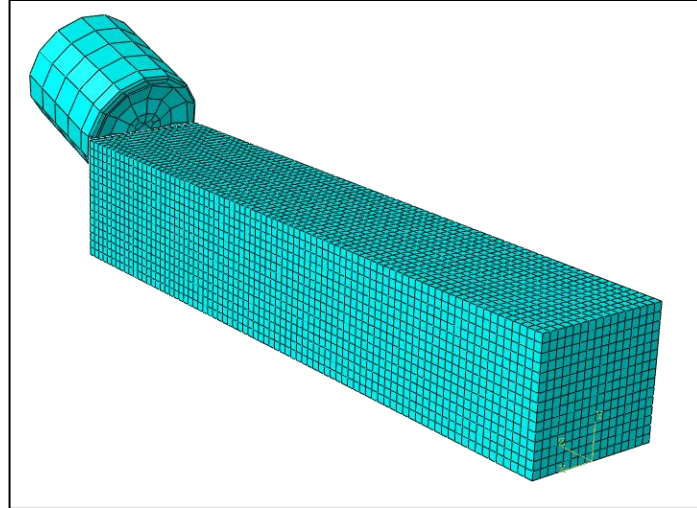
APPENDIX 1.2 Contour Plots for Different Cutter Back Rake Angle

20˚	30˚
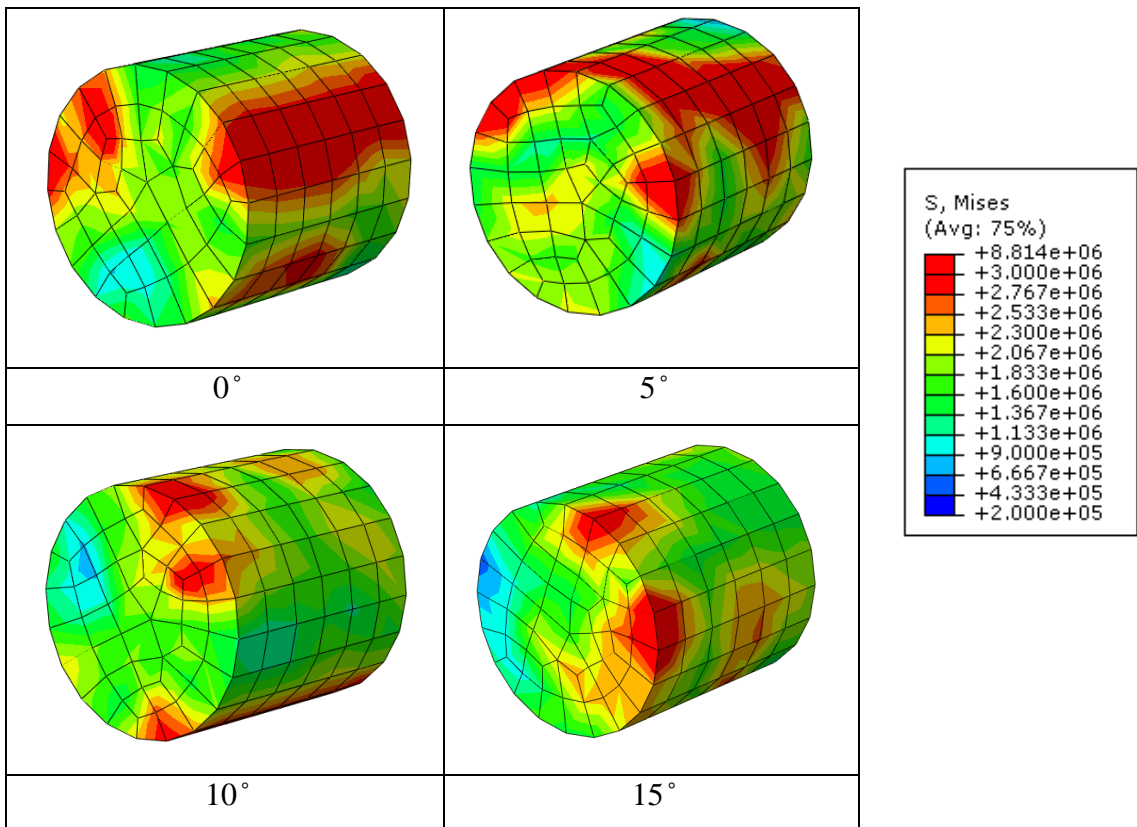
APPENDIX 1.3 Contour Plots for Different Shape of Cutter

Flat	Beveled	Multidimensional